Instability of a binary liquid film flowing down a slippery heated plate

E. Ellaban,[1,a)] J. P. Pascal,[1,b)] and S. J. D. D'Alessio[2,c)]
[1]*Department of Mathematics, Ryerson University, Toronto, Ontario M5B 2K3, Canada*
[2]*Department of Applied Mathematics, University of Waterloo, Waterloo, Ontario N2L 3G1, Canada*

(Received 9 June 2017; accepted 24 August 2017; published online 18 September 2017)

In this paper, we study the stability of a binary liquid film flowing down a heated slippery inclined surface. It is assumed that the heating induces concentration differences in the liquid mixture (Soret effect), which together with the differences in temperature affects the surface tension. A mathematical model is constructed by coupling the Navier-Stokes equations governing the flow with equations for the concentration and temperature. A Navier slip condition is applied at the liquid-solid interface. We carry out a linear stability analysis in order to obtain the critical conditions for the onset of instability. We use a Chebyshev spectral collocation method to obtain numerical solutions to the resulting Orr-Sommerfeld-type equations. We also obtain an asymptotic solution that yields an expression for the state of neutral stability of long perturbations as a function of the parameters controlling the problem. A weighted residual approximation is employed to derive a reduced model that is used to analyse the nonlinear effects. Good agreement between the linear stability analysis and nonlinear simulations provided by the weighted residual model is found. *Published by AIP Publishing.* [http://dx.doi.org/10.1063/1.4989558]

I. INTRODUCTION

Gravity-driven film flow is prone to interfacial instability resulting from the amplification of surface undulations due to inertial effects. The instability evolves into pronounced surface waves with important consequences in many applications. The ground-breaking experiments of Kapitza and Kapitza[1] provided important insight into the development of these waves. Both Benjamin[2] and Yih[3] have later carried out theoretical investigations based on the linear stability analysis of the fluid flow equations. Since then, theoretical models have been implemented which incorporate various extensions of the basic inclined flow problem. Of notable importance are nonisothermal flows for which thermocapillarity has a significant impact on the interfacial instability. Linear and nonlinear stability analyses have been carried out for inclined flows along heated surfaces. For these flows, thermocapillarity triggers two separate modes of instability: one is due to Marangoni stresses resulting from temperature perturbations along the surface and the other affects surface undulations. Specifically, the Marangoni stresses pull the fluid from the troughs to the crests of the waves where surface tension is stronger due to the distance from the heated substrate. This action amplifies the undulations and thus augments the inertial instability. Linear and nonlinear investigations of the instability of inclined heated film flow have been recently carried out by Kalliadasis *et al.*,[4] Ruyer-Quil *et al.*,[5] Scheid *et al.*,[6] and Trevelyan *et al.*[7]

In binary liquid mixtures, such as water and ethanol mixtures,[8] heating can also cause solutocapillarity. In particular, due to the Soret effect, temperature differences induce molecular fluxes leading to non-uniformity in the concentration of the solute. The impact of the Soret effect on the stability of horizontal layers has been extensively studied[9–14]. The inclined flow case has received considerably less attention. The first investigation of the problem was reported by Hu *et al.*,[15] who carried out a linear stability analysis. Just recently Pascal and D'Alessio[16] and D'Alessio and Pascal[17] have extended the investigation to account for buoyancy and accomplished both linear and nonlinear analyses.

Another practical modeling extension for inclined film flow is incorporating a slip condition at the liquid-solid boundary. Although the no-slip condition has become the default boundary condition applied at a solid-liquid interface, the validity of this condition was challenged at length during the nineteenth and early twentieth centuries. The notion of a slip condition was originally proposed by Navier.[18] Cases in which the no-slip condition is known to fail include the flows of rarified gases or flows within microfluidic/nanofluidic devices.[19] For situations involving hydrophobic solids or those with micro-structured surfaces, a more general Navier slip condition yields results that are in better agreement with experimental observations than the traditional no-slip condition.[20] Beavers and Joseph[21] proposed such a slip condition for a liquid-porous medium interface. Pascal[22] employed this condition in developing a one-sided model for flows down a porous incline. The accuracy of the one-sided model was examined by Liu and Liu[23] who concluded that using this approach generates more accurate results when the permeability is low or moderate, particularly if the porous substrate is sufficiently thin. Sadiq *et al.*[24] included thermocapillary effects into the one-sided model and studied the instability of flows down a heated permeable incline.

Using the reconstruction approaches of Sellier[25] and Heining and Aksel,[26] Usha and Anjalaiah[27] obtained steady solutions of thin-film flows over an uneven slippery incline.

[a)]Email: eglal.ellaban@ryerson.ca
[b)]Email: jpascal@ryerson.ca
[c)]Email: sdalessio@uwaterloo.ca

They analyzed the influence of inertia, slip, and surface tension on the shape of the reconstructed bottom for specific prescribed free surface shapes. Studies of flows involving two-layer systems down a slippery incline include the ones by Anjalaiah and Usha[28] and Gosh and Usha.[29] In Ref. 28 the stability of a two-layer immiscible fluid over a slippery bottom was investigated. They found that slip stabilizes the flow with or without the presence of surfactants along the air-liquid and liquid-liquid interfaces. On the other hand, in Ref. 29, the gravity-driven flow of a two-fluid miscible system along a slippery incline was studied. Again, the interesting result that emerged is that slip tends to stabilize the flow rather than destabilize the flow.

The aim of the present study is to incorporate the Soret effect and bottom slip in a theoretical model for investigating the stability of film flow down a heated incline. This paper is organized as follows. In Sec. II we establish the governing equations. In Sec. III a linear stability analysis is conducted. Numerical and asymptotic solutions are obtained for the associated eigenvalue problem and the effect of the various parameters on neutral stability is discussed. Nonlinear effects are considered in Sec. IV, while the conclusions of this study are summarized in Sec. V.

II. GOVERNING EQUATIONS

We consider the gravity-driven two-dimensional laminar flow of a binary liquid film over a uniformly heated slippery substrate inclined at an angle β with respect to the horizontal as shown in Fig. 1. An (x, z) rectangular coordinate system is established with the x-axis pointing down the incline and the z-axis pointing into the liquid layer. The velocity components in the x and z directions are given by u and w, respectively, while $z = h(x, t)$ is the position of the free surface. The temperature of the substrate is maintained at a prescribed constant value denoted by T_w, while the ambient gas that is assumed to remain motionless has a constant temperature $T_\infty < T_w$.

The equations of motion for the liquid film are obtained from the two-dimensional continuity and Navier-Stokes equations and are expressed as

$$\frac{\partial u}{\partial x} + \frac{\partial w}{\partial z} = 0, \tag{1}$$

$$\frac{\partial u}{\partial t} + u\frac{\partial u}{\partial x} + w\frac{\partial u}{\partial z} = -\frac{1}{\rho}\frac{\partial p}{\partial x} + g\sin\beta + \frac{\mu}{\rho}\left(\frac{\partial^2 u}{\partial x^2} + \frac{\partial^2 u}{\partial z^2}\right), \tag{2}$$

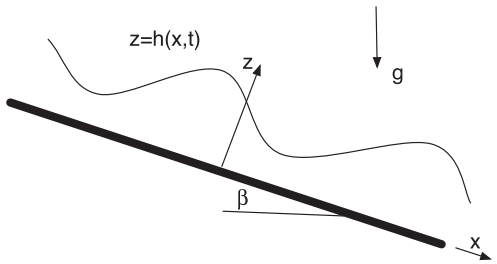

FIG. 1. Schematic representation of a thin film flowing down an inclined plane.

$$\frac{\partial w}{\partial t} + u\frac{\partial w}{\partial x} + w\frac{\partial w}{\partial z} = -\frac{1}{\rho}\frac{\partial p}{\partial z} - g\cos\beta + \frac{\mu}{\rho}\left(\frac{\partial^2 w}{\partial x^2} + \frac{\partial^2 w}{\partial z^2}\right), \tag{3}$$

where p is the pressure, g denotes the gravitational acceleration, while ρ and μ are the mass density and dynamic viscosity of the liquid mixture, respectively.

According to Fourier's law, the conductive heat flux is proportional to the temperature gradient, and similarly, by Fick's law, the mass flux is proportional to the concentration gradient. However, when both temperature and concentration differences exist, the heat and mass fluxes can be affected by both the temperature and concentration gradients. The dependence of the mass flux on the temperature gradient is referred to as the Soret effect, while the dependence of the heat flux on the concentration gradient is known as the Dufour effect. However, in liquid mixtures, only the Soret effect is significant. Consequently, the heat flux J_h and mass flux J_m will be expressed as

$$J_h = -\lambda\nabla T \quad \text{and} \quad J_m = -\rho\, D_m\left(\nabla C + \alpha\nabla T\right),$$

where C is the solute concentration, T is the temperature of the liquid mixture, $\lambda > 0$ is the thermal conductivity, $D_m > 0$ is the mass diffusivity, α is the Soret coefficient, and $\nabla = (\frac{\partial}{\partial x}, \frac{\partial}{\partial z})$. We point out that, depending on the nature of the binary liquid, the temperature-induced solute flux can be towards warmer or colder regions, and consequently, the Soret coefficient can take on negative or non-negative values.

Introducing the heat and mass fluxes into the basic advection-diffusion transport equation, we obtain the following equations governing the temperature and concentration:

$$\frac{\partial T}{\partial t} + u\frac{\partial T}{\partial x} + w\frac{\partial T}{\partial z} = \kappa\,\nabla^2 T, \tag{4}$$

$$\frac{\partial C}{\partial t} + u\frac{\partial C}{\partial x} + w\frac{\partial C}{\partial z} = D_m\left(\nabla^2 C + \alpha\nabla^2 T\right), \tag{5}$$

where κ is the thermal diffusivity.

We assume the viscous stress exerted by the ambient gas on the surface of the liquid layer to be negligible. Therefore, the force on the surface due to the flow is balanced by the ambient pressure and the effect of surface tension. The tangential component of the force balance at the surface is thus expressed as

$$\left[\frac{\partial\sigma}{\partial x} + \frac{\partial h}{\partial x}\left(\frac{\partial\sigma}{\partial z}\right)\right]\sqrt{1+\left(\frac{\partial h}{\partial x}\right)^2} = \mu\left[\left(1-\left(\frac{\partial h}{\partial x}\right)^2\right)\left(\frac{\partial u}{\partial z} + \frac{\partial w}{\partial x}\right) + 2\frac{\partial h}{\partial x}\left(\frac{\partial w}{\partial z} - \frac{\partial u}{\partial x}\right)\right] \quad \text{at} \quad z = h(x,t),$$

while the normal component is given by

$$p = p_\infty + \frac{2\mu}{1+\left(\frac{\partial h}{\partial x}\right)^2}\left[\left(\frac{\partial h}{\partial x}\right)^2\frac{\partial u}{\partial x} - \frac{\partial h}{\partial x}\left(\frac{\partial u}{\partial z} + \frac{\partial w}{\partial x}\right) + \frac{\partial w}{\partial z}\right] - \frac{\sigma\frac{\partial^2 h}{\partial x^2}}{\left(1+\left(\frac{\partial h}{\partial x}\right)^2\right)^{\frac{3}{2}}} \quad \text{at} \quad z = h(x,t),$$

where p_∞ is the ambient pressure and σ is the surface tension.

The surface tension is assumed to depend linearly on both the temperature and the solute concentration and is expressed as

$$\sigma = \sigma_\infty - \sigma_t (T - T_\infty) + \sigma_c (C - C_0),$$

where σ_∞ is the surface tension of the fluid at the reference values $T = T_\infty$ and $C = C_0$. The parameters σ_t and σ_c are defined as

$$\sigma_t = -\frac{\partial \sigma}{\partial T} \quad \text{and} \quad \sigma_c = \frac{\partial \sigma}{\partial C},$$

which are positive for nearly all binary liquids. So surface tension increases with concentration and decreases with temperature.

Assuming the liquid is non-volatile, a kinematic condition for the free surface is obtained based on negligible evaporation and is expressed as

$$w = \frac{\partial h}{\partial t} + \frac{\partial h}{\partial x} u \quad \text{at} \quad z = h(x,t).$$

The relation between the heat flux normal to the surface and the temperature difference can be expressed through Newton's law of cooling, which is given by

$$\chi \sqrt{1 + \left(\frac{\partial h}{\partial x}\right)^2} (T - T_\infty) = \lambda \left(\frac{\partial h}{\partial x} \frac{\partial T}{\partial x} - \frac{\partial T}{\partial z} \right) \quad \text{at} \quad z = h(x,t),$$

where χ is the heat transfer coefficient. Also, using the fact that the normal mass flux of the solute vanishes at the free surface, we obtain the boundary condition

$$-\frac{\partial h}{\partial x}\frac{\partial C}{\partial x} + \frac{\partial C}{\partial z} + \alpha \left(-\frac{\partial h}{\partial x}\frac{\partial T}{\partial x} + \frac{\partial T}{\partial z} \right) = 0 \quad \text{at} \quad z = h(x,t).$$

At the interface with the slippery substrate, we apply a Navier slip condition of the form

$$u = \gamma \frac{\partial u}{\partial z} \quad \text{at} \quad z = 0,$$

where γ is the slip length, and we take the normal component of velocity to be zero,

$$w = 0 \quad \text{at} \quad z = 0.$$

As a result, the normal solute flux is also zero, which is expressed as

$$\frac{\partial C}{\partial z} + \alpha \frac{\partial T}{\partial z} = 0 \quad \text{at} \quad z = 0.$$

And finally, since the substrate is maintained at temperature T_w, we have the condition

$$T = T_w \quad \text{at} \quad z = 0.$$

In order to nondimensionalize the governing equations, we employ the length scale

$$H = \left(\frac{3\mu Q}{\rho g \sin\beta} \right)^{\frac{1}{3}},$$

which is the Nusselt thickness of an isothermal flow along a non-slippery surface if the flow rate is prescribed to be Q. As a result, we will introduce the following transformation:

$$(x,z) = H(x^*, z^*), \quad h = Hh^*, \quad (u,w) = U(u^*, w^*),$$
$$t = \frac{H}{U} t^*, \quad p - p_\infty = \rho U^2 p^*, \quad T = T_\infty + \Delta T\, T^*,$$
$$C = C_0 + \frac{\sigma_t}{\sigma_c} \Delta T\, C^*,$$

where $U = Q/H$ and $\Delta T = T_w - T_\infty$. Applying this scaling and removing the asterisk for notational convenience, the conservation equations (1)–(5) become

$$\frac{\partial u}{\partial x} + \frac{\partial w}{\partial z} = 0, \tag{6}$$

$$Re\left(\frac{\partial u}{\partial t} + u\frac{\partial u}{\partial x} + w\frac{\partial u}{\partial z} \right) = -Re\frac{\partial p}{\partial x} + \frac{\partial^2 u}{\partial x^2} + \frac{\partial^2 u}{\partial z^2} + 3, \tag{7}$$

$$Re\left(\frac{\partial w}{\partial t} + u\frac{\partial w}{\partial x} + w\frac{\partial w}{\partial z} \right) = -Re\frac{\partial p}{\partial z} + \frac{\partial^2 w}{\partial x^2} + \frac{\partial^2 w}{\partial z^2} - 3\cot\beta, \tag{8}$$

$$PrRe\left(\frac{\partial T}{\partial t} + u\frac{\partial T}{\partial x} + w\frac{\partial T}{\partial z} \right) = \frac{\partial^2 T}{\partial x^2} + \frac{\partial^2 T}{\partial z^2}, \tag{9}$$

$$ScRe\left(\frac{\partial C}{\partial t} + u\frac{\partial C}{\partial x} + w\frac{\partial C}{\partial z} \right) = \frac{\partial^2 C}{\partial x^2} + \frac{\partial^2 C}{\partial z^2} + So\left(\frac{\partial^2 T}{\partial x^2} + \frac{\partial^2 T}{\partial z^2} \right), \tag{10}$$

where $Re = \frac{\rho Q}{\mu}$ is the Reynolds number, $\mathrm{Pr} = \frac{\mu}{\rho\kappa}$ is the Prandtl number, Sc is the Schmidt number given by $Sc = \frac{\nu}{D_m}$, and $So = \alpha \frac{\sigma_c}{\sigma_t}$ is the Soret number. It should be noted that fluid properties such as ρ, μ, κ and others will depend on temperature. The underlying assumption made here is that for reasonably small temperature differences $(T_w - T_\infty)$, these fluid properties will remain fairly constant. In previous studies,[16,17,30,31] the effects of having variable fluid properties have been investigated much more thoroughly. Applying the scaling to the continuity of normal stress condition at the free surface yields

$$p = \frac{2}{Re\left[1 + \left(\frac{\partial h}{\partial x}\right)^2\right]} \left[\left(\frac{\partial h}{\partial x}\right)^2 \frac{\partial u}{\partial x} - \frac{\partial h}{\partial x}\left(\frac{\partial w}{\partial x} + \frac{\partial u}{\partial z} \right) + \frac{\partial w}{\partial z} \right] - \frac{We - M(T - C)}{\left(1 + \left(\frac{\partial h}{\partial x}\right)^2\right)^{\frac{3}{2}}} \frac{\partial^2 h}{\partial x^2} \quad \text{at} \quad z = h(x,t), \tag{11}$$

where the dimensionless parameters M and the Weber number, We, are defined as

$$M = \frac{\sigma_t \Delta T}{\rho U^2 H} \quad \text{and} \quad We = \frac{\sigma_\infty}{\rho U^2 H}.$$

Scaling the continuity of the tangential stress condition at the free surface leads to

$$-MRe\sqrt{1 + \left(\frac{\partial h}{\partial x}\right)^2} \left[\frac{\partial (T - C)}{\partial x} + \frac{\partial h}{\partial x}\left(\frac{\partial (T - C)}{\partial z} \right) \right] = \left[1 - \left(\frac{\partial h}{\partial x}\right)^2 \right] \left(\frac{\partial w}{\partial x} + \frac{\partial u}{\partial z} \right) - 4\frac{\partial h}{\partial x}\frac{\partial u}{\partial x} \quad \text{at} \quad z = h(x,t). \tag{12}$$

The kinematic condition transforms into

$$w = \frac{\partial h}{\partial t} + u\frac{\partial h}{\partial x} \quad \text{at} \quad z = h(x,t). \tag{13}$$

Applying the scaling to Newton's law of cooling yields

$$BT\sqrt{1+\left(\frac{\partial h}{\partial x}\right)^2}=\left(\frac{\partial h}{\partial x}\right)\left(\frac{\partial T}{\partial x}\right)-\frac{\partial T}{\partial z}\quad\text{at}\quad z=h(x,t),\quad(14)$$

where $B=\frac{\chi H}{\lambda}$. The zero mass flux condition at the free surface and at the bottom is scaled as

$$-\left(\frac{\partial h}{\partial x}\right)\left(\frac{\partial C}{\partial x}\right)+\frac{\partial C}{\partial z}+So\left[-\left(\frac{\partial h}{\partial x}\right)\left(\frac{\partial T}{\partial x}\right)+\frac{\partial T}{\partial z}\right]=0\quad\text{at}\quad z=h(x,t),\quad(15)$$

$$\frac{\partial C}{\partial z}+So\frac{\partial T}{\partial z}=0\quad\text{at}\quad z=0.\quad(16)$$

The remaining boundary conditions at $z=0$ are nondimensionalized to give

$$u=\delta\frac{\partial u}{\partial z}\quad\text{at}\quad z=0,\quad(17)$$

$$w=0,\quad T=1\quad\text{at}\quad z=0,\quad(18)$$

where $\delta=\frac{\gamma}{H}$ is the scaled slip length.

III. LINEAR STABILITY ANALYSIS

The problem (6)–(18) governing a falling binary liquid film along a slippery heated inclined plate admits a simple solution corresponding to a steady uniform flow in the streamwise direction. This equilibrium solution is obtained by solving the problem under the assumption of x and t independence. Equations (6)–(10) then reduce to

$$\frac{\partial w}{\partial z}=0,\quad\frac{\partial^2 u}{\partial z^2}=-3,\quad\frac{\partial p}{\partial z}=-3\frac{\cot\beta}{Re},$$

$$\frac{\partial^2 T}{\partial z^2}=0\quad\text{and}\quad\frac{\partial^2 C}{\partial z^2}=0,$$

while at $z=h_s$, the conditions are given by

$$\frac{\partial u}{\partial z}=0,\quad p=0,\quad\frac{\partial C}{\partial z}+So\frac{\partial T}{\partial z}=0,\quad\text{and}\quad\frac{\partial T}{\partial z}=-BT,$$

where h_s is the equilibrium thickness of the liquid film. At $z=0$, the conditions become

$$\delta\frac{\partial u}{\partial z}=u,\quad w=0,\quad T=1,\quad\text{and}\quad\frac{\partial C}{\partial z}+So\frac{\partial T}{\partial z}=0.$$

At $z=0$ we can, without loss of generality, also impose the condition $C=0$. This corresponds to setting the reference concentration C_0 to be the concentration at the plate induced by the Soret effect.

As a result, the equilibrium solution can be written as

$$w=w_s(z)\equiv 0,$$

$$u=u_s(z)\equiv-\frac{3}{2}z^2+3h_sz+3\delta h_s,$$

$$p=p_s(z)\equiv-3\frac{\cot\beta}{Re}(z-h_s),$$

$$T=T_s(z)\equiv 1-\left(\frac{B}{1+Bh_s}\right)z,$$

and

$$C=C_s(z)\equiv So\left(\frac{B}{1+Bh_s}\right)z.$$

In order for the equilibrium flow rate to equal the prescribed value, we have the constraint

$$\int_0^{h_s}u_s(z)dz=1,$$

which yields

$$h_s^3+3\delta h_s^2-1=0,\quad(19)$$

and solving for h_s, we obtain the equilibrium thickness of the liquid layer as

$$h_s=\frac{1}{2}\left(4-8\delta^3+4\sqrt{-4\delta^3+1}\right)^{\frac{1}{3}}+\frac{2\delta^2}{\left(4-8\delta^3+4\sqrt{-4\delta^3+1}\right)^{\frac{1}{3}}}-\delta.\quad(20)$$

We express the perturbed equilibrium solution as follows:

$$h=h_s+\eta(x,t),\quad u=u_s(z)+\tilde{u}(x,z,t),\quad w=\tilde{w}(x,z,t),$$

$$p=p_s(z)+\tilde{p}(x,z,t),\quad T=T_s(z)+\tilde{T}(x,z,t),\quad\text{and}$$

$$C=C_s(z)+\tilde{C}(x,z,t),$$

where η, $\tilde{u}$, $\tilde{w}$, $\tilde{p}$, $\tilde{T}$, and $\tilde{C}$ are the added infinitesimal perturbations. We introduce this perturbed state into Eqs. (6)–(10) and then linearize with respect to the perturbation variables to obtain

$$\frac{\partial\tilde{u}}{\partial x}+\frac{\partial\tilde{w}}{\partial z}=0,\quad(21)$$

$$Re\left(\frac{\partial\tilde{u}}{\partial t}+u_s\frac{\partial\tilde{u}}{\partial x}+\tilde{w}\frac{du_s}{dz}\right)=-Re\frac{\partial\tilde{p}}{\partial x}+\frac{\partial^2\tilde{u}}{\partial x^2}+\frac{\partial^2\tilde{u}}{\partial z^2},\quad(22)$$

$$Re\left(\frac{\partial\tilde{w}}{\partial t}+u_s\frac{\partial\tilde{w}}{\partial x}\right)=-Re\frac{\partial\tilde{p}}{\partial z}+\frac{\partial^2\tilde{w}}{\partial x^2}+\frac{\partial^2\tilde{w}}{\partial z^2},\quad(23)$$

$$PrRe\left(\frac{\partial\tilde{T}}{\partial t}+u_s\frac{\partial\tilde{T}}{\partial x}+\tilde{w}\frac{dT_s}{dz}\right)=\frac{\partial^2\tilde{T}}{\partial x^2}+\frac{\partial^2\tilde{T}}{\partial z^2},\quad(24)$$

and

$$ScRe\left(\frac{\partial\tilde{C}}{\partial t}+u_s\frac{\partial\tilde{C}}{\partial x}+\tilde{w}\frac{dC_s}{dz}\right)=\frac{\partial^2\tilde{C}}{\partial x^2}+\frac{\partial^2\tilde{C}}{\partial z^2}+So\left(\frac{\partial^2\tilde{T}}{\partial x^2}+\frac{\partial^2\tilde{T}}{\partial z^2}\right).\quad(25)$$

Transferring the boundary conditions at $z=h_s+\eta$ to $z=h_s$ and linearizing yield the following conditions at $z=h_s$:

$$\tilde{p}-3\frac{\cot\beta}{Re}\eta-\frac{2}{Re}\frac{\partial\tilde{w}}{\partial z}+(We-M(T_s-C_s))\frac{\partial^2\eta}{\partial x^2}=0,\quad(26)$$

$$-MRe\left[\frac{\partial\tilde{T}}{\partial x}-\frac{\partial\tilde{C}}{\partial x}-\frac{B(1+So)}{1+Bh_s}\frac{\partial\eta}{\partial x}\right]=\frac{\partial\tilde{w}}{\partial x}+\frac{\partial\tilde{u}}{\partial z}-3\eta,\quad(27)$$

$$\frac{\partial \tilde{C}}{\partial z} + So\frac{\partial \tilde{T}}{\partial z} = 0, \tag{28}$$

$$\tilde{w} = \frac{\partial \eta}{\partial t} + u_s\frac{\partial \eta}{\partial x}, \tag{29}$$

and

$$\frac{\partial \tilde{T}}{\partial z} = \frac{B^2\eta}{1+Bh_s} - B\tilde{T}. \tag{30}$$

At $z = 0$, the conditions are

$$\frac{\partial \tilde{C}}{\partial z} + So\frac{\partial \tilde{T}}{\partial z} = 0, \tag{31}$$

$$\tilde{u} = \delta\frac{\partial \tilde{u}}{\partial z}, \tag{32}$$

and

$$\tilde{w} = \tilde{T} = 0\,. \tag{33}$$

We next employ normal modes into the linearized perturbation equations which are defined as

$$\left(\tilde{u}, \tilde{w}, \tilde{p}, \tilde{T}, \tilde{C}, \eta\right) = \left(\hat{u}(z), \hat{w}(z), \hat{p}(z), \hat{T}(z), \hat{C}(z), \hat{\eta}\right) e^{ik(x-ct)},$$

where k represents the perturbation wavenumber which is a real positive number, c is a complex quantity whose real part gives the phase speed of the perturbation, while the product of the imaginary part and k equals the growth rate. Then the linearized perturbation equations (21)–(33) can be written as

$$D\hat{w} + ik\hat{u} = 0\,, \tag{34}$$

$$Re\left[ik\left(u_s - c\right)\hat{u} + Du_s\hat{w}\right] = -ikRe\hat{p} + D^2\hat{u} - k^2\hat{u}, \tag{35}$$

$$ikRe\left(u_s - c\right)\hat{w} = -ReD\hat{p} + D^2\hat{w} - k^2\hat{w}, \tag{36}$$

$$PrRe\left[ik\left(u_s - c\right)\hat{T} + DT_s\hat{w}\right] = D^2\hat{T} - k^2\hat{T}, \tag{37}$$

$$ScRe\left[ik\left(u_s - c\right)\hat{C} + DC_s\hat{w}\right] = D^2\hat{C} - k^2\hat{C} + So\left(D^2\hat{T} - k^2\hat{T}\right), \tag{38}$$

$$\hat{p} - \frac{3}{Re}\cot\beta\hat{\eta} - \frac{2}{Re}D\hat{w} - k^2\left[We - M\left(1 - \frac{Bh_s(1+So)}{1+Bh_s}\right)\right]\hat{\eta} = 0 \quad \text{at} \quad z = h_s, \tag{39}$$

$$-ikMRe\left[\hat{T} - \hat{C} - \frac{B(1+So)}{1+Bh_s}\hat{\eta}\right] = -3\hat{\eta} + D\hat{u} + ik\hat{w} \quad \text{at} \quad z = h_s, \tag{40}$$

$$D\hat{C} + SoD\hat{T} = 0 \quad \text{at} \quad z = h_s, \tag{41}$$

$$\hat{w} = ik(u_s - c)\hat{\eta} \quad \text{at} \quad z = h_s, \tag{42}$$

$$D\hat{T} = \frac{B^2}{1+Bh_s}\hat{\eta} - B\hat{T} \quad \text{at} \quad z = h_s, \tag{43}$$

$$\hat{w} = \hat{T} = 0 \quad \text{at} \quad z = 0, \tag{44}$$

$$D\hat{C} + SoD\hat{T} = 0 \quad \text{at} \quad z = 0, \tag{45}$$

and

$$\hat{u} = \delta D\hat{u} \quad \text{at} \quad z = 0, \tag{46}$$

where D denotes the differentiation with respect to the z operator. The quantity $\hat{p}$ can be eliminated from Eqs. (35), (36), (39), and (34) is automatically satisfied if we introduce the stream function ψ, which is related to the velocity perturbation by

$$\tilde{u} = \frac{\partial \psi}{\partial z},\ \tilde{w} = -\frac{\partial \psi}{\partial x}.$$

In terms of the normal modes, ψ can be written as

$$\psi = \Psi(z)e^{ik(x-ct)},$$

in which case $\hat{u}$ and $\hat{w}$ can be expressed as

$$\hat{u} = D\Psi,\ \hat{w} = -ik\Psi.$$

Consequently, we have the following Orr-Sommerfeld-type equations:

$$D^4\Psi - \left[ikRe\left(u_s - c\right) + 2k^2\right]D^2\Psi + \left[ik^3Re\left(u_s - c\right) + k^4 - 3ikRe\right]\Psi = 0, \tag{47}$$

$$D^2\hat{T} - k^2\hat{T} - PrRe\left[ik\left(u_s - c\right)\hat{T} + ik\left(\frac{B}{1+Bh_s}\right)\Psi\right] = 0, \tag{48}$$

$$D^2\hat{C} - k^2\hat{C} - ScRe\left[ik\left(u_s - c\right)\hat{C} - ik\frac{SoB}{1+Bh_s}\Psi\right] + So\left(D^2\hat{T} - k^2\hat{T}\right) = 0. \tag{49}$$

The boundary conditions at $z = h_s$ are

$$D^3\Psi - \left[ikRe\left(u_s - c\right) + 3k^2\right]D\Psi - \left[3ik\cot\beta + ik^3Re\left(We - M\left(\frac{1 - Bh_sSo}{1+Bh_s}\right)\right)\right]\hat{\eta} = 0, \tag{50}$$

$$D^2\Psi + k^2\Psi + ikMRe\left(\hat{T} - \hat{C}\right) - \left(3 + ikMRe\frac{B(1+So)}{1+Bh_s}\right)\hat{\eta} = 0, \tag{51}$$

$$D\hat{C} + SoD\hat{T} = 0, \tag{52}$$

$$\left(u_s - c\right)\hat{\eta} + \Psi = 0, \tag{53}$$

$$D\hat{T} + B\hat{T} - \frac{B^2}{1+Bh_s}\hat{\eta} = 0. \tag{54}$$

The conditions at $z = 0$ are

$$\Psi = \hat{T} = 0, \tag{55}$$

$$D\hat{C} + SoD\hat{T} = 0, \tag{56}$$

$$\delta D^2\Psi - D\Psi = 0. \tag{57}$$

The problem given by Eqs. (47)–(57) constitutes an eigenvalue problem with c being the parameter that is to be assigned characteristic values. Solving for c provides the growth rate of the perturbation with wavenumber k for a given set of flow parameters $(Re, \mathrm{Pr}, B, Sc, So, M, \beta, \delta, We)$. A positive value of $\Im(c)$ indicates that the perturbation amplitude grows in time, while if $\Im(c)$ is negative, then the perturbation is damped. A set of flow parameters for which $\Im(c) = 0$ is referred to as the state of neutral stability for the perturbation with wavenumber k and corresponds to the threshold between stability and instability for this perturbation. Regarding the stability of the flow, if all the perturbations are damped, then the flow is stable, otherwise it is unstable.

The solution of the eigenvalue problem (47)–(57) can be obtained by carrying out an asymptotic analysis as $k \to 0$. First, we expand the perturbations $\Psi, \hat{T}, \hat{C}, \hat{\eta}$ and the eigenvalue c in powers of k as follows:

$$\begin{aligned}
\Psi &= \Psi_0(z) + ik\Psi_1(z) + O(k^2),\\
\hat{T} &= \hat{T}_0(z) + ik\hat{T}_1(z) + O(k^2),\\
\hat{C} &= \hat{C}_0(z) + ik\hat{C}_1(z) + O(k^2),\\
\hat{\eta} &= \hat{\eta}_0 + ik\hat{\eta}_1 + O(k^2),\\
c &= c_0 + ikc_1 + O(k^2).
\end{aligned}$$

Substituting into the system of Eqs. (47)–(57) and assuming all parameters to be $O(1)$ as $k \to 0$, we can construct a hierarchy of problems at different orders of k for the undetermined factors in the expansions. These quantities will be real and thus the growth rate of a perturbation with wavenumber k will be $k^2 c_1$, with the state of neutral stability then being given by $c_1 = 0$. In solving these problems, we found $\hat{\eta}_0$ to be arbitrary and the relation for neutral stability to be independent of $\hat{\eta}_1$. Therefore we present the results for $\hat{\eta}_0 = 1$ and $\hat{\eta}_1 = 0$.

Collecting the leading-order terms, we obtain

$$D^4\Psi_0 = 0, \quad D^2\hat{T}_0 = 0, \quad D^2\hat{C}_0 = 0,$$

with boundary conditions at $z = h_s$ being

$$\begin{aligned}
D^3\Psi_0(h_s) &= 0,\\
D^2\Psi_0(h_s) - 3 &= 0,\\
D\hat{C}_0(h_s) + SoD\hat{T}_0(h_s) &= 0,\\
u_s(h_s) - c_0 + \hat{\Psi}_0(h_s) &= 0,\\
D\hat{T}_0(h_s) + B\hat{T}_0(h_s) - \frac{B^2}{1+Bh_s} &= 0,
\end{aligned}$$

and the boundary conditions at $z = 0$ being

$$\begin{aligned}
\Psi_0(0) = \hat{T}_0(0) &= 0,\\
D\hat{C}_0(0) + SoD\hat{T}_0(0) &= 0,\\
\delta D^2\Psi_0(0) - D\Psi_0(0) &= 0.
\end{aligned}$$

The solution to this problem is easily obtained and given by

$$\begin{aligned}
\Psi_0 &= \frac{3}{2}z^2 + 3\delta z,\\
\hat{T}_0 &= \frac{B^2}{(1+Bh_s)^2}z,\\
c_0 &= 3h_s\,(2\delta + h_s)\,,\\
\hat{C}_0 &= -\frac{SoB^2}{(1+Bh_s)^2}z + C_{00},
\end{aligned}$$

where the constant C_{00} is determined from the $O(k)$ problem. Specifically, if we take the $O(k)$ terms in Eq. (49), we obtain

$$D^2\hat{C}_1 + SoD^2\hat{T}_1 = ScRe\left[\left(-\frac{3}{2}z^2 + 3h_s z + 3\delta h_s - c_0\right)\hat{C}_0 - \frac{SoB}{1+Bh_s}\Psi_0\right],$$

and from conditions (52) and (56), we get

$$D\hat{C}_1 + SoD\hat{T}_1 = 0 \quad \text{at} \quad z = 0 \quad \text{and} \quad z = h_s.$$

Integrating the differential equation yields an expression for $D\hat{C}_1 + SoD\hat{T}_1$, which we introduce into the conditions and find that

$$C_{00} = \frac{BSoh_s(-24B\delta h_s - 9Bh_s^2 + 4Bc_0 - 12\delta - 4h_s)}{8(Bh_s+1)^2(-3\delta h_s - h_s^2 + c_0)}.$$

At $O(k)$, we obtain the following system of equations for Ψ_1:

$$\begin{aligned}
D^4\Psi_1(z) - Re\big(u_s(z) - c_0\big)D^2\Psi_0(z) - 3Re\Psi_0(z) &= 0,\\
D^3\Psi_1(h_s) - Re\big(u_s(h_s) - c_0\big)D\Psi_0(h_s) - 3\cot\beta &= 0,\\
D^2\Psi_1(h_s) + MRe\big(\hat{T}_0(h_s) - \hat{C}_0(h_s)\big) - MRe\frac{B(So+1)}{(Bh_s+1)} &= 0,\\
\Psi_1(h_s) - c_1 &= 0,\\
\Psi_1(0) &= 0,\\
\delta D^2\Psi_1(0) - D\Psi_1(0) &= 0.
\end{aligned} \tag{58}$$

We obtained an explicit solution for Ψ_1 by means of the Maple symbolic algebra software; however, the expression is very long and presenting it is not useful.

From condition (58), we have $c_1 = \Psi_1(h_s)$, and so the neutral stability relation is given by $\Psi_1(h_s) = 0$, which can be solved for Re to give the following expression for the critical Reynolds number:

$$\begin{aligned}
Re_{crit} = \Big(&80(3\delta + h_s)\cot\beta\, h_s(3B^2\delta h_s^2 + 2B^2h_s^3 + 6B\delta h_s + 4Bh_s^2 + 3\delta + 2h_s)\Big)\Big/\\
&\Big(2160B^2\delta^4h_s^4 + 5040B^2\delta^3h_s^5 + 4128B^2\delta^2h_s^6 + 1440B^2\delta h_s^7 + 192B^2h_s^8 + 4320B\delta^4h_s^3\\
&+ 10080B\delta^3h_s^4 + 8256B\delta^2h_s^5 + 2880B\delta h_s^6 + 384Bh_s^7 + 30B^2MSo\delta h_s^2 + 15B^2MSoh_s^3\\
&+ 2160\delta^4h_s^2 + 5040\delta^3h_s^3 + 4128\delta^2h_s^4 + 1440\delta h_s^5 + 192h_s^6 + 120BMSo\delta^2 + 180BMSo\delta h_s\\
&+ 60BMSoh_s^2 + 240BM\delta^2 + 280BM\delta h_s + 80BMh_s^2\Big).
\end{aligned} \tag{59}$$

For the no-slip case, $\delta = 0$, this expression reduces to

$$Re_{crit} = \frac{10(1+B)^2 \cot\beta}{12(1+B)^2 + \frac{5}{12}MB(16+12So+3SoB)}, \quad (60)$$

which is in full agreement with the result obtained by Hu *et al.*,[15] provided the difference in scaling is taken into account. The Soret effect can be discarded by setting $So = 0$, in which case we obtain

$$Re_{crit} = \frac{5}{6}\cot\beta\left[\frac{(h_s+3\delta)h_s}{\frac{1}{2}h_s^2(\delta+h_s)(2h_s^2+10\delta h_s+15\delta^2)+\frac{5MB(h_s+2\delta)}{12(1+Bh_s)^2}}\right]. \quad (61)$$

If we use the thickness of the equilibrium flow as the length scale, in which case $h_s = 1$, this expression for the critical Reynolds number takes the form

$$Re_{crit} = \frac{5}{6}\cot\beta\left[\frac{(1+3\delta)}{1+6\delta+\frac{25}{2}\delta^2+\frac{15}{2}\delta^3+\frac{5MB(1+2\delta)}{12(1+B)^2}}\right], \quad (62)$$

which coincides with the result found by Sadiq *et al.*[24] If we set $M = So = \delta = 0$, our expression reduces to $Re_{crit} = \frac{5}{6}\cot\beta$, which is the well known isothermal result obtained by Benjamin[2] and Yih.[3]

It is important to mention that the asymptotic analysis only determines the instability of very long perturbations. Consequently, it does not accurately predict the onset of instability if shorter perturbations are the most unstable ones. As it was discovered by Pascal and D'Alessio,[16] this is the case if capillarity and the Soret effect are sufficiently strong and the Soret coefficient is negative.

In order to determine the growth rate of perturbations in general, we must resort to a numerical method to solve the eigenvalue problem (47)–(57). We employed a collocation method based on polynomial interpolation with Chebyshev points.[32] Accordingly, we introduced the expansions

$$\Psi = \sum_{j=0}^{N} w_j P_j(\xi), \quad \hat{T} = \sum_{j=0}^{N} v_j P_j(\xi), \quad \hat{C} = \sum_{j=0}^{N} u_j P_j(\xi),$$

where $\xi = \frac{2}{h_s}z - 1$ and

$$P_j(\xi) = \frac{\prod_{\substack{n=0\\n\neq j}}^{N}(\xi-\xi_n)}{\prod_{\substack{n=0\\n\neq j}}^{N}(\xi_j-\xi_n)}, \quad j = 0,1,2,\ldots,N,$$

with $\xi_l = -\cos\left(\frac{l\pi}{N}\right)$, $l = 0,\ 1,\ 2,\ldots,\ N$. This leads to an algebraic system of the form

$$\mathcal{A}y = c\mathcal{B}y,$$

where

$$y = [w_0\ w_1\ \cdots\ w_N\ v_0\ v_1\ \cdots\ v_N\ u_0\ u_1\ \cdots\ u_N\ \hat{\eta}]^T$$

and $\mathcal{A}$ and $\mathcal{B}$ are $(3N+4)\times(3N+4)$ matrices. The eigenvalues of this system were calculated using the Matlab subroutine **eig**. The correct eigenvalue for the differential problem (47)–(57) was determined by recalculating the eigenvalues of the algebraic system for a finer grid and identifying the value that remained unchanged.

It turns out that the parameters We, M, and B are implicitly dependent on the Reynolds number. Thus, in order to determine the solution for the critical Reynolds number, we introduce new parameters Ka, Ma, and Bi related to the previous ones by $We = \left(\frac{3}{\sin\beta}\right)^{1/3}\frac{Ka}{Re^{5/3}}$, $M = \left(\frac{3}{\sin\beta}\right)^{1/3}\frac{Ma}{Re^{5/3}}$, and $B = \left(\frac{3}{\sin\beta}\right)^{1/3} BiRe^{1/3}$, where $Ka = \frac{\sigma_\infty \rho^{1/3}}{g^{1/3}\mu^{4/3}}$ is the Kapitza number, $Ma = \frac{\sigma_t \Delta T \rho^{1/3}}{g^{1/3}\mu^{4/3}}$ is the Marangoni number, and $Bi = \frac{\gamma\mu^{2/3}}{\lambda g^{1/3}\rho^{2/3}}$ is the Biot number.

In terms of the new parameters, depending on the prescribed values, the asymptotic expression for neutral stability yields either two real positive roots for the critical Reynolds number or no such solutions. The two roots correspond to the so-called S and H modes of instability. For small Reynolds numbers, inertial forces are insufficient to amplify waves on the surface of the liquid layer. However, the equilibrium flow may still be unstable due to fluid motion induced by Marangoni stresses resulting from surface tension variation caused by perturbations in temperature and solute concentration. The amplification of perturbations much longer than the thickness of the layer by this type of instability is referred to as the S mode. With sufficiently strong inertia, perturbations in the elevation of the liquid surface may be amplified and may lead to hydrodynamic instability referred to as the H mode. Thermocapillary and solutocapillary effects can enhance the instability of the H mode if the variation in surface tension results in stronger levels at the crests of surface waves than at the troughs. Marangoni stresses then pull the fluid toward the crests thus amplifying the amplitude. As the destabilizing effect of capillarity is intensified, both modes are destabilized; the minimum amount of inertia that will stabilize the S mode increases, and the maximum level of inertia that will allow surface undulations to be damped decreases. These two measures will eventually coincide at which point the equilibrium flow is unstable for all Reynolds numbers. Our aim in this investigation is to study the stability of the equilibrium flow and we thus consider parameter values that correspond to the separate evolution of the two modes of instability up to conditions when they merge. In order to demonstrate that these cases correspond to real fluids and describe flows encountered in applications, we first discuss the realistic ranges for our parameters.

Hu *et al.*[15] indicated that the Soret coefficient ranges from -10^{-2} to 10^{-2}, while the ratio σ_c/σ_t is of the order 10^2, and consequently typical values of the Soret number lie between -1 and 1. They also specified that the molecular diffusive process in binary liquids is such that typically $10^2 Pr \le Sc \le 10^4 Pr$. In accordance with this restriction, in our investigations, we have set $Pr = 7$ and $Sc = 700$.

In order to demonstrate that the parameter values that we considered are associated with temperature differences that are consistent with the assumption made about negligible evaporation and constant fluid properties, we present an example from the experimental findings reported by Khattab *et al.*[33] for

aqueous solutions of ethanol. These measurements indicate that for a mixture that is approximately 17% ethanol, at a temperature of 293 K, the viscosity is $\mu = 2.62\times10^{-3} Pa\,s$, the density is $\rho = 9.47\times10^{2}\ kg/m^3$, and the rate of change in surface tension with temperature can estimated to be $\sigma_t \approx 9\times10^{-5}\ \frac{N}{K\,m}$. Now, in the results that we present, in order to capture the merging of the two modes of instability, we must increase the Marangoni number up to approximately $Ma = 2.5$. The corresponding temperature difference then is

$$\Delta T = \frac{Ma\, g^{1/3}\mu^{4/3}}{\sigma_t \rho^{1/3}} = 2.18\times10^{-3} K.$$

Also, from the data presented by Khattab *et al.*,[33] we deduce that the rates of change in viscosity and density are approximately $\frac{\Delta\mu}{\Delta T} \approx -6.58\times10^{-5} s\,Pa/K$ and $\frac{\Delta\rho}{\Delta T} \approx -1.08\,\frac{kg}{m^3 K}$, respectively. For the specified temperature difference, the resulting scaled variations in viscosity and density then are of the order 10^{-5}, which is small enough to justify the approximation that these quantities are temperature independent. We also point out that this example is comparable to the one presented by Podolny *et al.*[12] who also employ a model that assumes negligible evaporation and constant fluid properties. These same assumptions are also made by Hu *et al.*[15] with actually much larger Marangoni numbers; up to order 10^2. In obtaining their results, they fixed the inclination at 15°, while we chose a steeper slope at 45° in our investigation. The reduced inclination taken by Hu *et al.*[15] results in a significantly larger critical Reynolds number for the H mode, and consequently stronger thermocapillarity is required to decrease this value and increase the critical Reynolds number of the S mode to the point where the two coincide.

Regarding applications with flows over hydrophobic surfaces exhibiting microscopic texture, the dimensioned slip length can range up to the order of micrometres.[19] Now, we must assume the film layer to be sufficiently thick so that inertial effects are relevant, yet thin enough to render the variations in the fluid properties with temperature negligible. The appropriate range would extend from tens of micrometres to about 1 *mm*.[34] The resulting values for the scaled slip length, δ, would then range up to values of order 10^{-1}. This agrees with the range indicated by Anjalaiah and Usha[28] and the values considered by Samanta *et al.*[35]

The same order of magnitude for δ applies when the substrate is composed of a porous material. In this case, the dimensioned slip length is given by $\gamma = \frac{\sqrt{\Pi}}{\Lambda}$, where Π is the permeability and Λ is the Beavers-Joseph constant. Λ takes values from 0.1 to 0.4,[21] while for common porous materials, $\sqrt{\Pi}$ extends from very small numbers to values comparable to 10^{-2} *mm*.[36] Sadiq *et al.*[24] focused on an example with $\sqrt{\Pi} = 8.58\times10^{-2}$ *mm* and $H = 2.4$ *mm* for the characteristic thickness of the liquid layer. Allowing the Beavers-Joseph constant to range over the specified values, they thus considered the interval from 0.0089 to 0.3575 for the scaled slip length δ. The results that we present below correspond to δ values from 0 to 0.4.

Neutral stability curves in the $k - Re$ plane are shown in Figs. 2–5. The intercepts with the Re-axis correspond to the critical Reynolds number for the onset of instability of perturbations with $k = 0$. These are in excellent agreement with the result from the asymptotic analysis when the parameters are $O(1)$. The results reveal that as Ma is increased, both the S and H modes are destabilized and the two modes eventually merge indicating that the equilibrium flow is unstable for all Reynolds numbers. The parameter Ma is a measure of thermocapillarity, so as it is increased, temperature perturbations cause greater surface tension variation that destabilizes the flow. Furthermore, if the free surface is undulated, then the troughs are warmer than the crests due to their

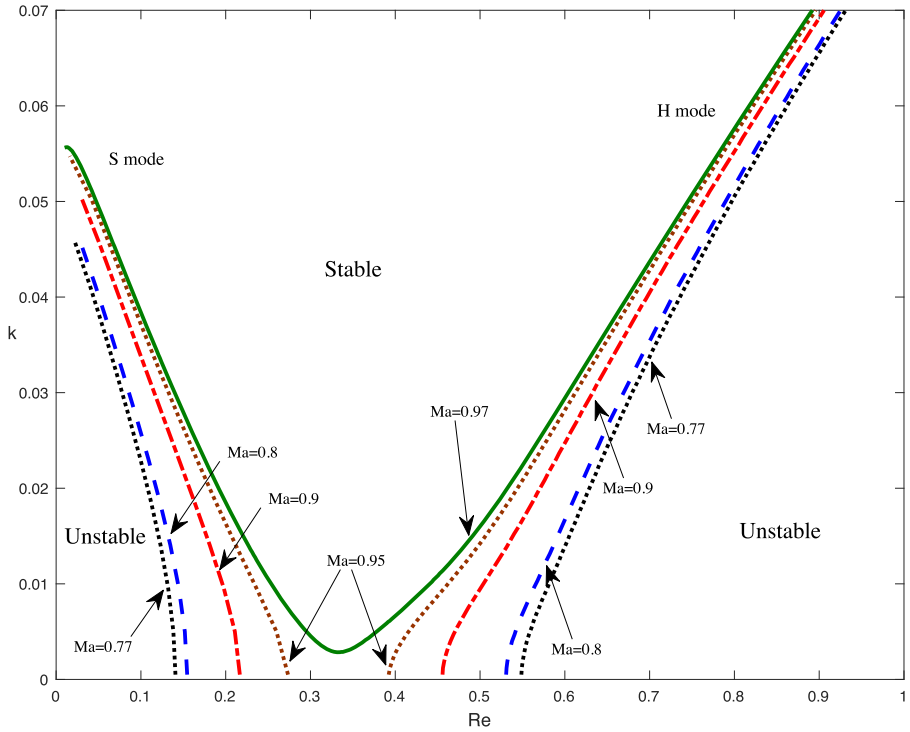

FIG. 2. Neutral stability curves for different values of Ma with $\cot\beta = 1$, $Pr = 7$, $Bi = 1$, $Ka = 100$, $Sc = 700$, $So = 0.5$, and $\delta = 0$.

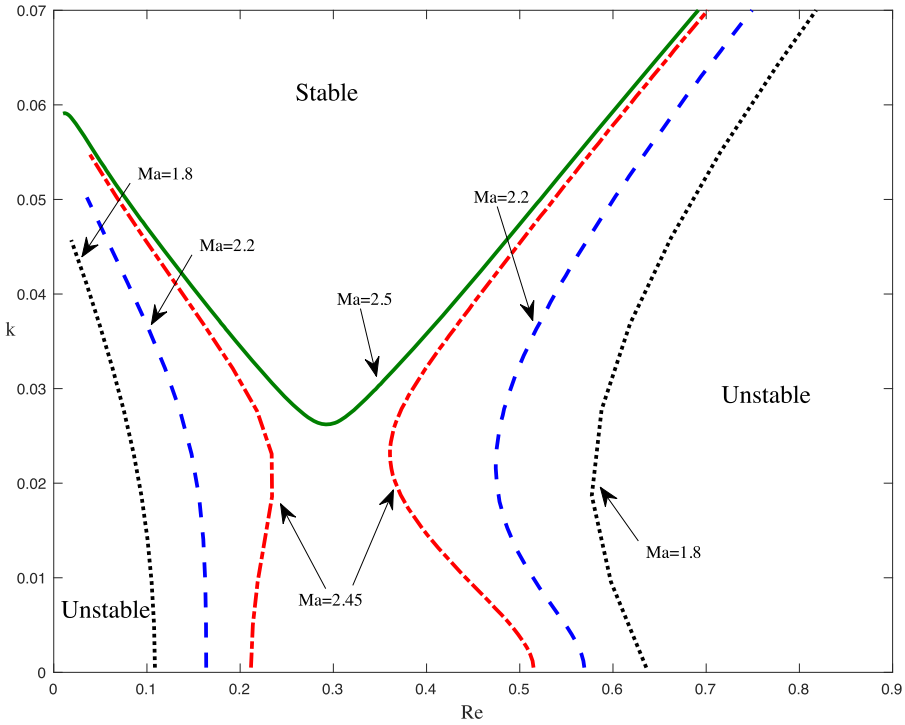

FIG. 3. Neutral stability curves for different values of Ma with $\cot\beta = 1$, $Pr = 7$, $Bi = 1$, $Ka = 100$, $Sc = 700$, $So = -0.5$, and $\delta = 0$.

proximity to the heated bottom. As a result, surface tension is stronger at the crests and thus the resulting Marangoni stresses act to amplify the undulations and as such the H mode is destabilized.

The results in Figs. 2 and 3 correspond to $\delta = 0$ (the no-slip case). Note that in Fig. 2 the onset of instability of the equilibrium flow is due to the amplification of infinitely long perturbations. However, as it was also observed by Pascal and D'Alessio,[16] it turns out that if So is negative and is of sufficiently large absolute value, as Ma is increased, the curves for both the S and the H modes develop a "nose" profile as it can be seen in Fig. 3. This means that there is a band of moderately long perturbations that are the most unstable and the instability of the flow is due to the amplification of these perturbations as opposed to the infinitely long ones. The results in Figs. 4 and 5 correspond to a case with a slippery bottom for positive and negative values of So, respectively. As it can be seen, like in the no-slip case, with negative So, instability of the equilibrium flow is due to perturbations of finite wavelength. However, it is noticeable that if the substrate is slippery, the nose structure

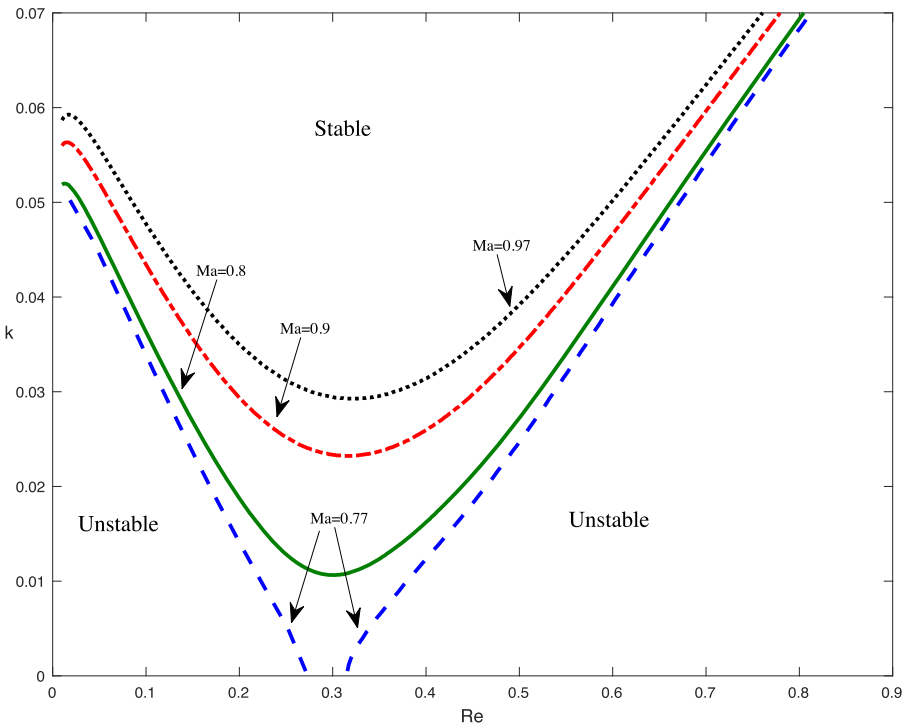

FIG. 4. Neutral stability curves for different values of Ma with $\cot\beta = 1$, $Pr = 7$, $Bi = 1$, $Ka = 100$, $Sc = 700$, $So = 0.5$, and $\delta = 0.2$.

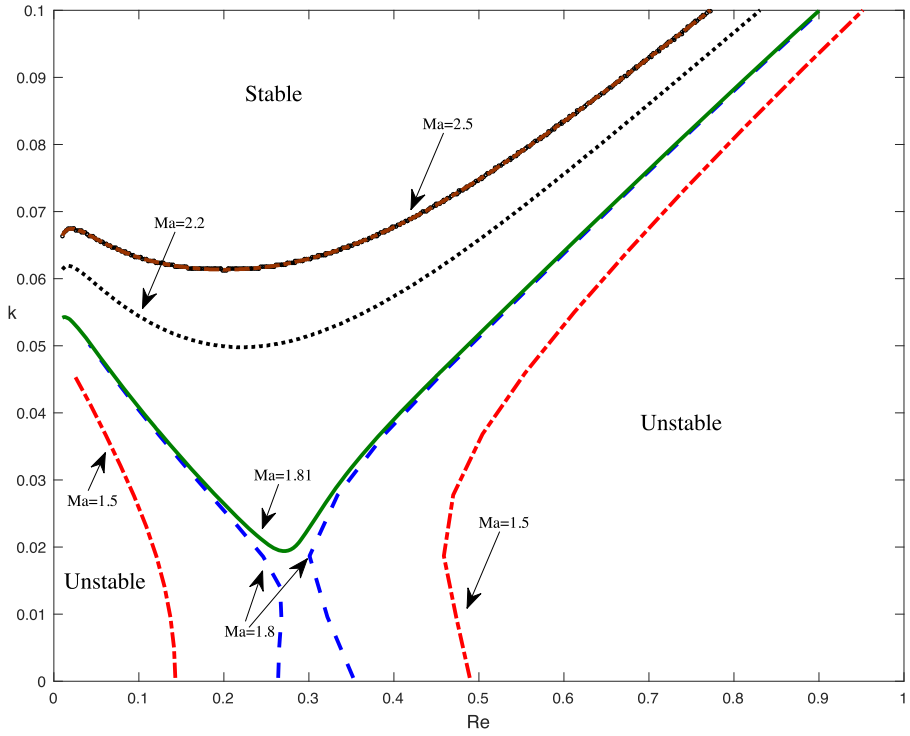

FIG. 5. Neutral stability curves for different values of Ma with $\cot\beta = 1$, $Pr = 7$, $Bi = 1$, $Ka = 100$, $Sc = 700$, $So = -0.5$, and $\delta = 0.2$.

is less pronounced, there being a smaller difference between the critical Reynolds number for the onset of instability and that for which perturbations with $k = 0$ become unstable. This is due to the fact that the S and H modes merge at a lower Marangoni number resulting in a shorter range of values for the nose to develop.

Another observation from the neutral stability curves is that for a given Marangoni number, the interval of Reynolds numbers for which the flow is stable is smaller if δ is non-zero, suggesting that bottom slip is a destabilizing factor. To better determine how slip affects the stability of the flow, in Fig. 6 we display the critical Reynolds number as a function of Ma for different values of δ. The upper branch of the curve describes the onset of the instability of the H mode, while the S mode is described by the lower branch of the curve, and the region inside the curve indicates the Reynolds numbers for which the flow is stable. It can be seen that the region of stability shrinks as δ is increased, and as a result, we conclude that increasing the slip length destabilizes the flow for both the S and H modes. These conclusions are the same as those

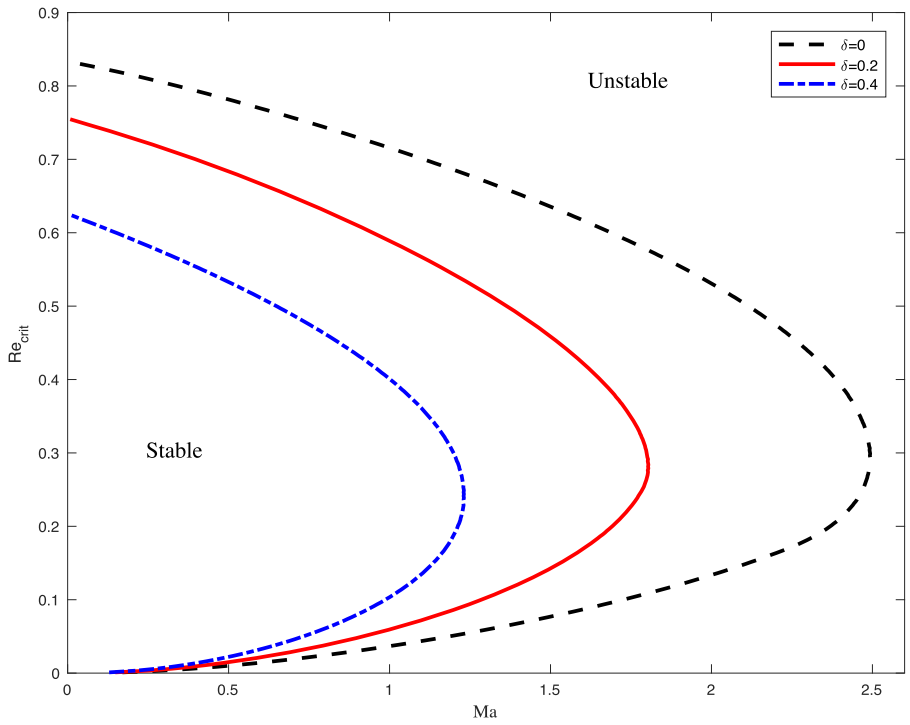

FIG. 6. Re_{crit} as a function of Ma with $\cot\beta = 1$, $Pr = 7$, $Bi = 1$, $Ka = 100$, $Sc = 700$, and $So = -0.5$.

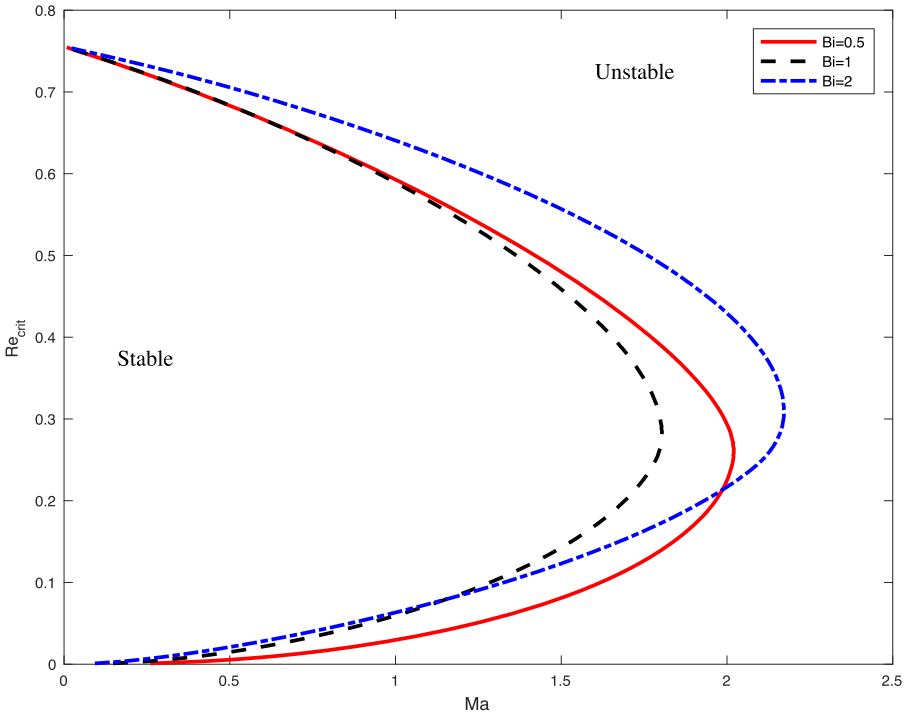

FIG. 7. Re_{crit} as a function of Ma with $\cot\beta = 1$, $Pr = 7$, $Ka = 100$, $Sc = 700$, $So = -0.5$, and $\delta = 0.2$.

drawn by Sadiq *et al.*[24] for the thermo-porous problem without the Soret effect.

The effect of the Biot number on the critical Reynolds number is illustrated in Fig. 7. With $Bi = 0$, the equilibrium temperature in the fluid layer, including the surface, is constant. As a result, the surface temperature and the concentration of the solute are uniform. Consequently, the Marangoni effect and the Soret effect are neutralized. On the other hand, for large Biot numbers, the surface temperature approaches that of the ambient gas which is constant, and as such the Marangoni effect and the Soret effect are again neutralized. Therefore, there is a critical Biot number at which the temperature and concentration variations, and consequently that in surface tension, are at their greatest. For this value of the Biot number, the Marangoni effect is maximized resulting in the most unstable flow. As it is illustrated in Fig. 7, when Bi increases from zero, the region of stability shrinks, reaches a minimum, and then increases. As a result, we conclude that the S and H modes both experience a destabilizing effect with small values of Bi and a stabilizing one with sufficiently large values of Bi.

Figure 8 shows Re_{crit} versus Ma for different values of the Soret number holding the other flow parameters constant.

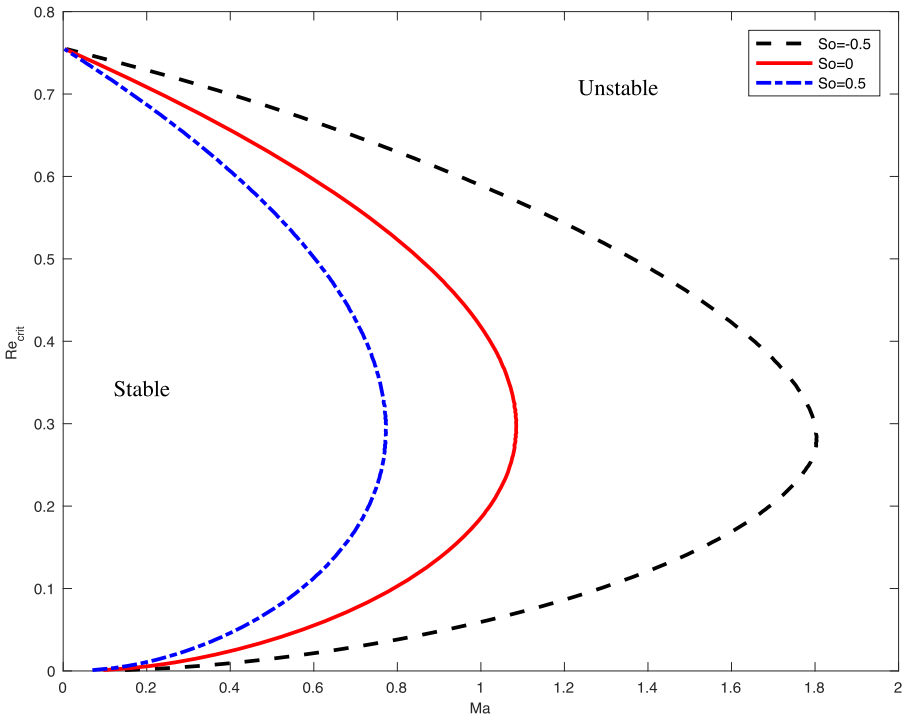

FIG. 8. Re_{crit} as a function of Ma with $\cot\beta = 1$, $Pr = 7$, $Bi = 1$, $Ka = 100$, $Sc = 700$, and $\delta = 0.2$.

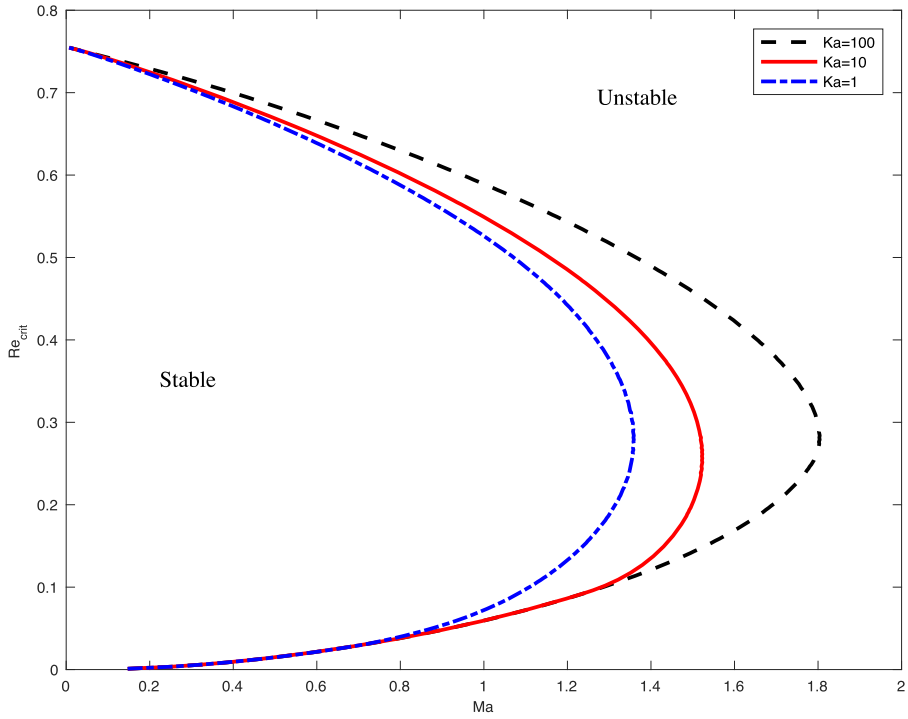

FIG. 9. Re_{crit} as a function of Ma with $\cot\beta = 1$, $Pr = 7$, $Bi = 1$, $Sc = 700$, $So = -0.5$, and $\delta = 0.2$.

The results indicate that increasing the Soret number destabilizes the flow. More specifically, if So is positive, increasing the magnitude of the Soret effect, measured by the absolute value of So, destabilizes the flow, and if So is negative, increasing the Soret effect stabilizes it. In fact, increasing the magnitude of the Soret effect results in greater concentration differences induced by temperature perturbations and thus amplifies the Marangoni stresses. However, if So is negative, a mass flux is induced towards warmer regions, and as a result, we have a higher concentration of solute at the troughs of surface perturbations than at the crests. But surface tension increases with concentration, so, with negative values of So, the Soret effect acts to increase surface tension at the troughs and lower it at the crests, which acts to dampen surface undulations and stabilize the flow.

We next consider the effect of the magnitude of the surface tension which is measured by the Kapitza number. Now, it is well known that surface tension dampens surface waves, but it has very little effect on very long waves. For cases when So is positive, we do not expect any effect of the Kapitza number on the onset of instability since it is due to the amplification of infinitely long perturbations. For cases when So is negative, like the one considered in Fig. 9, the onset of instability is due to perturbations of finite wavelength. So the region of stability increases with Ka.

IV. NONLINEAR EFFECTS

In this section, we investigate the effect of nonlinearity on the stability of the flow. To this end, we implement a reduced model where the explicit dependence on the vertical coordinate is eliminated by applying a weighted residual technique. The weighted residual approach was originally applied by Ruyer-Quil and Manneville[37,38] to handle isothermal flows down an even incline. It has since then been applied to more complicated flows. For example, Kalliadasis *et al.*[4] extended the weighted residual method to model flows down an even heated incline, D'Alessio *et al.*[39] used it to model isothermal flows over a wavy incline, while D'Alessio and Pascal[40] successfully applied it to inclined isothermal flows down an uneven porous surface. Further extensions include heated flows over wavy[41] and porous wavy inclines.[42] Recently, D'Alessio and Pascal[17] successfully applied the weighted residual technique to a flow model with the no-slip condition which includes the Soret effect.

In order to extend the weighted residual technique to include thermosolutal capillarity, we first introduce slow time and space variables, τ and X, respectively, and rescale the vertical velocity according to

$$\tau = \varepsilon t,\ X = \varepsilon x,\ w = \varepsilon W,$$

where $0 < \varepsilon \ll 1$ is a small parameter. Then the scaled conservation equations (6)–(10) become

$$\varepsilon\left(\frac{\partial u}{\partial X} + \frac{\partial W}{\partial z}\right) = 0, \tag{63}$$

$$\varepsilon Re\left(\frac{\partial u}{\partial \tau} + u\frac{\partial u}{\partial X} + W\frac{\partial u}{\partial z}\right) = -\varepsilon Re\frac{\partial p}{\partial X} + 3 + \varepsilon^2\frac{\partial^2 u}{\partial X^2} + \frac{\partial^2 u}{\partial z^2}, \tag{64}$$

$$\varepsilon^2 Re\left(\frac{\partial W}{\partial \tau} + u\frac{\partial W}{\partial X} + W\frac{\partial W}{\partial z}\right) = -Re\frac{\partial p}{\partial z} - 3\cot\beta + \varepsilon^3\frac{\partial^2 W}{\partial X^2} + \varepsilon\frac{\partial^2 W}{\partial z^2}, \tag{65}$$

$$\varepsilon PrRe\left(\frac{\partial T}{\partial \tau} + u\frac{\partial T}{\partial X} + W\frac{\partial T}{\partial z}\right) = \varepsilon^2\frac{\partial^2 T}{\partial X^2} + \frac{\partial^2 T}{\partial z^2}, \tag{66}$$

$$\varepsilon ScRe\left(\frac{\partial C}{\partial \tau}+u\frac{\partial C}{\partial X}+W\frac{\partial C}{\partial z}\right)=\varepsilon^2\frac{\partial^2 C}{\partial X^2}+\frac{\partial^2 C}{\partial z^2}+So\left(\varepsilon^2\frac{\partial^2 T}{\partial X^2}+\frac{\partial^2 T}{\partial z^2}\right), \quad (67)$$

and are equivalent to the long-wave equations.

The transformed boundary conditions at $z = h(x, t)$ are

$$p=\frac{2}{ReF}\left(\varepsilon^2\left[\frac{\partial h}{\partial X}\right]^2\frac{\partial u}{\partial X}+\varepsilon\frac{\partial W}{\partial z}-\varepsilon\frac{\partial h}{\partial X}\left[\frac{\partial u}{\partial z}+\varepsilon^2\frac{\partial W}{\partial X}\right]\right)-\varepsilon^2\frac{[We-M(T-C)]}{F^{3/2}}\frac{\partial^2 h}{\partial X^2}, \quad (68)$$

$$-MRe\sqrt{F}\left[\varepsilon\frac{\partial}{\partial X}(T-C)+\varepsilon\frac{\partial h}{\partial X}\frac{\partial}{\partial z}(T-C)\right]=G\left(\frac{\partial u}{\partial z}+\varepsilon^2\frac{\partial W}{\partial X}\right)-4\varepsilon^2\frac{\partial h}{\partial X}\frac{\partial u}{\partial X}, \quad (69)$$

$$\varepsilon W=\varepsilon\left(\frac{\partial h}{\partial \tau}+u\frac{\partial h}{\partial X}\right), \quad (70)$$

$$-B\sqrt{F}T=\frac{\partial T}{\partial z}-\varepsilon^2\frac{\partial h}{\partial X}\frac{\partial T}{\partial X}, \quad (71)$$

$$\frac{\partial C}{\partial z}-\varepsilon^2\frac{\partial h}{\partial X}\frac{\partial C}{\partial X}+So\left(\frac{\partial T}{\partial z}-\varepsilon^2\frac{\partial h}{\partial X}\frac{\partial T}{\partial X}\right)=0, \quad (72)$$

while the bottom conditions at $z = 0$ are

$$W=\frac{\partial C}{\partial z}+So\frac{\partial T}{\partial z}=0,\quad T=1,\quad \delta\frac{\partial u}{\partial z}=u, \quad (73)$$

and

$$F=1+\varepsilon^2\left[\frac{\partial h}{\partial X}\right]^2,\quad G=1-\varepsilon^2\left[\frac{\partial h}{\partial X}\right]^2.$$

The basic idea behind the weighted residual method is to eliminate the z dependence by assuming specific profiles for the velocity, temperature, and solutal concentration. We propose the following:

$$u=\frac{3q}{2(h^3+3\delta h^2)}b+\frac{\varepsilon MRe(1+So)}{4h}b_1\frac{\partial\theta}{\partial X},$$

$$T=1+\frac{(\theta-1)}{h}z,$$

$$C=-\frac{So(\theta-1)}{h}z,$$

where b, b_1 are given by

$$b=z(2h-z)+2\delta h,\quad b_1=z(2h-3z),$$

which can be viewed as basis functions with respect to the z–coordinate. Here, the interfacial temperature is denoted by $\theta(x,t) = T(x, z = h, t)$ and

$$q=\int_0^h u\,dz$$

is the flow rate. The u profile was chosen so as to satisfy the slip condition in (73) to $O(\varepsilon\delta)$ and the free-surface condition (69) to $O(\varepsilon)$, which when combined with the assumed profiles becomes

$$\frac{\partial u}{\partial z}=-\varepsilon MRe(1+So)\frac{\partial\theta}{\partial X}\quad \text{at}\quad z=h.$$

Although the profile for T satisfies the bottom condition $T = 1$ at $z = 0$, it does not satisfy the free-surface condition (71). In fact, it is impossible for the profile to satisfy both. However, as noted by Kalliadasis *et al.*,[4] the free-surface condition is incorporated into the energy equation when it is integrated over the fluid thickness, as described below. Lastly, it is worth pointing out that the solutal concentration can be expressed in terms of the temperature and satisfies all the boundary conditions. Because of this, the solutal concentration equation becomes redundant as C can be computed from the temperature.

In accordance with the Galerkin approach, we take b as the weight function and multiply Eq. (64) by b and integrate with respect to z from 0 to h. The pressure term in Eq. (64) is eliminated by using Eq. (65) as follows. First, we discard the $O(\varepsilon^2)$ terms to obtain

$$\frac{\partial p}{\partial z}=-\frac{3\cot\beta}{Re}+\frac{\varepsilon}{Re}\frac{\partial^2 W}{\partial z^2}.$$

This is then integrated from z to h and the boundary condition at $z = h$ is applied to yield an expression for the pressure which is then substituted into Eq. (64). Since the pressure term in Eq. (64) is multiplied by ε, the $O(\varepsilon^2)$ terms in Eq. (65) are discarded. This will result in a second-order weighted residual model. For the energy equation, we take the weight function to be z and multiply Eq. (66) by this and again integrate from 0 to h. After some algebra, we obtain the following equations for the flow variables h, q, and θ:

$$\frac{\partial h}{\partial \tau}+\frac{\partial q}{\partial X}=0, \quad (74)$$

$$\frac{\partial q}{\partial \tau}+\frac{\partial}{\partial X}\left[\frac{9}{7}\frac{q^2}{h}+\frac{5\cot\delta}{4Re}h^2+\frac{5}{4}M(1+So)\theta\right]=\frac{q}{7h}\left(\frac{h+18\delta}{h+11\delta}\right)\frac{\partial q}{\partial X}-\frac{5\cot\beta}{2Re}\left(\frac{\delta}{h+11\delta}\right)h\frac{\partial h}{\partial X}+\frac{5}{2\varepsilon Re}\left(h-\frac{q}{h^2}\right)$$
$$+\frac{5}{2\varepsilon Re}\left(\frac{\delta}{h+11\delta}\right)\left(h+\frac{2q}{h^2}\right)+\frac{135}{2\varepsilon Re}\left(\frac{\delta^2}{h+11\delta}\right)\left(2-\frac{q}{h^3}\right)$$
$$+\frac{\varepsilon}{Re}\left(\frac{h}{h+11\delta}\right)\left[\frac{9}{2}\frac{\partial^2 q}{\partial X^2}-\frac{9}{2h}\frac{\partial q}{\partial X}\frac{\partial h}{\partial X}+\frac{4q}{h^2}\left(\frac{\partial h}{\partial X}\right)^2-\frac{6q}{h}\frac{\partial^2 h}{\partial X^2}\right]$$
$$+\frac{\varepsilon ReM(1+So)}{16}\left(\frac{h}{h+11\delta}\right)\left[\frac{h^2}{3}\frac{\partial^2\theta}{\partial X\partial\tau}+\frac{15hq}{14}\frac{\partial^2\theta}{\partial X^2}+\frac{19h}{21}\frac{\partial q}{\partial X}\frac{\partial\theta}{\partial X}+\frac{5q}{7}\frac{\partial h}{\partial X}\frac{\partial\theta}{\partial X}\right], \quad (75)$$

$$h\frac{\partial\theta}{\partial\tau}+\frac{27q}{20}\frac{\partial\theta}{\partial X}-\frac{7}{40}(1-\theta)\frac{\partial q}{\partial X}=\frac{3}{\varepsilon RePr}\left(1+\frac{3\delta}{h}\right)^2\left[\frac{1-(1+Bh)\theta}{h+6\delta}\right]+\frac{21\delta q}{20(h+6\delta)}\frac{\partial\theta}{\partial X}-\frac{21\delta(1-\theta)}{40(h+6\delta)}\frac{\partial q}{\partial X}+\frac{21\delta q(1-\theta)}{40h(h+6\delta)}\frac{\partial h}{\partial X}$$
$$+\frac{\varepsilon}{RePr}\left(\frac{h}{h+6\delta}\right)\left[(1-\theta)\frac{\partial^2 h}{\partial X^2}+h\frac{\partial^2\theta}{\partial X^2}+\frac{\partial h}{\partial X}\frac{\partial\theta}{\partial X}-\left(\frac{3B\theta}{2}-\frac{(1-\theta)}{h}\right)\left(\frac{\partial h}{\partial X}\right)^2\right]$$
$$+\frac{3\varepsilon ReM(1+So)}{80}\left(\frac{h}{h+6\delta}\right)\left[2h^2\left(\frac{\partial\theta}{\partial X}\right)^2-h^2(1-\theta)\frac{\partial^2\theta}{\partial X^2}-2h(1-\theta)\frac{\partial h}{\partial X}\frac{\partial\theta}{\partial X}\right]. \tag{76}$$

In arriving at these equations, we have assumed that the parameters $Re, M, B, \Pr, We, So$, and $\cot\beta$ are all of order unity. In addition, we have only retained terms up to $O(\varepsilon^2)$, $O(\delta^2)$, and $O(\varepsilon\delta)$. Note that if we assume We to be $O(1)$, then the effect of the magnitude of surface tension drops from the equations.

If we perform a linear stability analysis on system (74)–(76) with $\delta = 0$, we obtain

$$Re_{crit}=\frac{10(1+B)^2\cot\beta}{12(1+B)^2+5MB(1+So)}.$$

This formula is in agreement with the asymptotic analysis of the linearized full equations described in Sec. III when the constant $\hat{C}_{00} = 0$. As explained by D'Alessio and Pascal,[16] this quantity must be set to zero since in the weighted residual model, the solute concentration is not explicitly included in the problem and hence perturbations to its equilibrium state are not included in the stability analysis.

Excellent agreement in Re_{crit} values between the linearized weighted residual equations (using $\varepsilon = 0.1$) and the full equations was also found in the slippery bottom case. Shown in Fig. 10 is a comparison for the case $B = 1.333$, $\cot\beta = 1$, $So = 0.5$, $Sc = 1$, $\delta = 0.1$, and $\Pr = 7$ over the range $0 \le M \le 10$. We also include Re_{crit} values in this plot obtained from nonlinear simulations using the numerical solution procedure which we now outline.

We begin by expressing governing Eqs. (74)–(76) in terms of the flow variables h, q, and $\Phi = h(\theta - 1)$. From the relation $(T-1)h = (\theta-1)z$, it follows that the variable Φ is related to T through

$$\int_0^h (T-1)dz=\frac{\Phi}{2},$$

and thus, Φ is proportional to the linear heat content stored in the fluid layer. Equations (74)–(76) then become

$$\frac{\partial h}{\partial\tau}+\frac{\partial q}{\partial X}=0, \tag{77}$$

$$\frac{\partial q}{\partial\tau}+\frac{\partial}{\partial X}\left[\frac{9}{7}\frac{q^2}{h}+\frac{5}{4}\frac{\cot\beta}{Re}h^2+\frac{5}{4}M(1+So)\frac{\Phi}{h}\right]=\frac{q}{7h}\left(\frac{h+18\delta}{h+11\delta}\right)\frac{\partial q}{\partial X}-\frac{5\cot\beta}{2Re}\left(\frac{\delta}{h+11\delta}\right)h\frac{\partial h}{\partial X}+\frac{5}{2\varepsilon Re}\left(h-\frac{q}{h^2}\right)$$
$$+\frac{5}{2\varepsilon Re}\left(\frac{\delta}{h+11\delta}\right)\left(h+\frac{2q}{h^2}\right)+\frac{135}{2\varepsilon Re}\left(\frac{\delta^2}{h+11\delta}\right)\left(2-\frac{q}{h^3}\right)$$
$$+\frac{\varepsilon}{Re}\left(\frac{h}{h+11\delta}\right)\left[\frac{9}{2}\frac{\partial^2 q}{\partial X^2}-\frac{9}{2h}\frac{\partial q}{\partial X}\frac{\partial h}{\partial X}+\frac{4q}{h^2}\left(\frac{\partial h}{\partial X}\right)^2-\frac{6q}{h}\frac{\partial^2 h}{\partial X^2}\right]$$
$$+\frac{\varepsilon ReM(1+So)}{48}\left(\frac{h}{h+11\delta}\right)\left[h\frac{\partial^2\Phi}{\partial X\partial\tau}-\frac{\partial h}{\partial X}\frac{\partial\Phi}{\partial\tau}+\frac{26}{7}\frac{\partial q}{\partial X}\frac{\partial\Phi}{\partial X}+\phi\frac{\partial^2 q}{\partial X^2}\right]$$
$$+\frac{\varepsilon ReM(1+So)}{112}\left(\frac{h}{h+11\delta}\right)\left[-10\frac{q}{h}\frac{\partial h}{\partial X}\frac{\partial\Phi}{\partial X}+10\frac{q\Phi}{h^2}\left(\frac{\partial h}{\partial X}\right)^2\right.$$
$$\left.-11\frac{\Phi}{h}\frac{\partial h}{\partial X}\frac{\partial q}{\partial X}+\frac{15}{2}q\frac{\partial^2\Phi}{\partial X^2}-\frac{15}{2}\frac{q\Phi}{h}\frac{\partial^2 h}{\partial X^2}\right], \tag{78}$$

$$\frac{\partial\Phi}{\partial\tau}+\frac{\partial}{\partial X}\left[\frac{27}{20}\frac{q\Phi}{h}\right]=\frac{7\Phi}{40h}\frac{\partial q}{\partial X}-\frac{3}{\varepsilon RePr(h+6\delta)}\left(1+\frac{3\delta}{h}\right)^2\left(B(h+\Phi)+\frac{\Phi}{h}\right)$$
$$+\frac{21\delta q}{20h(h+6\delta)}\frac{\partial\Phi}{\partial X}+\frac{21\delta\Phi}{40h(h+6\delta)}\frac{\partial q}{\partial X}-\frac{63\delta q\Phi}{40h^2(h+6\delta)}\frac{\partial h}{\partial X}$$
$$+\frac{3\varepsilon ReM(1+So)}{80}\left(\frac{h}{h+6\delta}\right)\left[\Phi\frac{\partial^2\Phi}{\partial X^2}+2\left(\frac{\partial\Phi}{\partial X}\right)^2-\frac{4\Phi}{h}\frac{\partial h}{\partial X}\frac{\partial\Phi}{\partial X}-\frac{\Phi^2}{h}\frac{\partial^2 h}{\partial X^2}+\frac{2\Phi^2}{h^2}\left(\frac{\partial h}{\partial X}\right)^2\right]$$
$$+\frac{\varepsilon}{RePr}\left(\frac{h}{h+6\delta}\right)\left[\frac{\partial^2\Phi}{\partial X^2}-\frac{1}{h}\frac{\partial h}{\partial X}\frac{\partial\Phi}{\partial X}-\frac{2\Phi}{h}\frac{\partial^2 h}{\partial X^2}-\frac{3B}{2}\left(1+\frac{\Phi}{h}\right)\left(\frac{\partial h}{\partial X}\right)^2\right]. \tag{79}$$

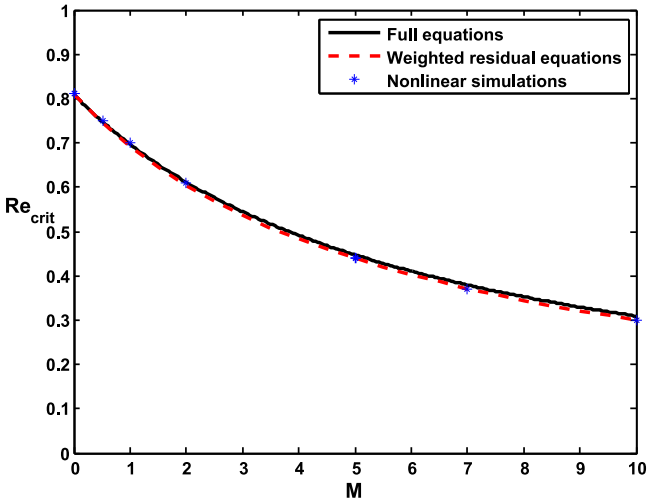

FIG. 10. Comparison in Re_{crit}.

The solutal concentration can be computed using

$$C = -\frac{So\Phi}{h^2}z.$$

To numerically solve the system of Eqs. (77)–(79), we first express these equations in the form

$$\frac{\partial h}{\partial \tau} + \frac{\partial q}{\partial X} = 0,$$

$$\frac{\partial q}{\partial \tau} + \frac{\partial}{\partial X}\left[\frac{9}{7}\frac{q^2}{h} + \frac{5}{4}\frac{\cot\beta}{Re}h^2 + \frac{5}{4}M(1+So)\frac{\Phi}{h}\right] = S_1 + \chi_1,$$

$$\frac{\partial \Phi}{\partial \tau} + \frac{\partial}{\partial X}\left[\frac{27}{20}\frac{q\Phi}{h}\right] = S_2 + \chi_2,$$

where the source terms S_1, S_2 are given by

$$S_1 = \frac{5}{2\varepsilon Re}\left(h - \frac{q}{h^2}\right) + \frac{5}{2\varepsilon Re}\left(\frac{\delta}{h+11\delta}\right)\left(h + \frac{2q}{h^2}\right) + \frac{135}{2\varepsilon Re}\left(\frac{\delta^2}{h+11\delta}\right)\left(2 - \frac{q}{h^3}\right),$$

$$S_2 = -\frac{3}{\varepsilon RePr(h+6\delta)}\left(1 + \frac{3\delta}{h}\right)^2\left(B(h+\Phi) + \frac{\Phi}{h}\right),$$

and χ_1 and χ_2 can be easily determined from (78) and (79). To solve this system of equations, the fractional-step splitting technique[43] was implemented. We first discard the derivative source terms and solve

$$\frac{\partial h}{\partial \tau} + \frac{\partial q}{\partial X} = 0,$$

$$\frac{\partial q}{\partial \tau} + \frac{\partial}{\partial X}\left[\frac{9}{7}\frac{q^2}{h} + \frac{5}{4}\frac{\cot\beta}{Re}h^2 + \frac{5}{4}M(1+So)\frac{\Phi}{h}\right] = S_1(h,q,\Phi),$$

$$\frac{\partial \Phi}{\partial \tau} + \frac{\partial}{\partial X}\left[\frac{27}{20}\frac{q\Phi}{h}\right] = S_2(h,\Phi),$$

over a time step $\Delta\tau$, and then solve

$$\frac{\partial q}{\partial \tau} = \chi_1\left(h, q, \Phi, \frac{\partial h}{\partial X}, \frac{\partial q}{\partial X}, \frac{\partial \Phi}{\partial X}, \frac{\partial \Phi}{\partial \tau}, \frac{\partial^2 h}{\partial X^2}, \frac{\partial^2 q}{\partial X^2}, \frac{\partial^2 \Phi}{\partial X^2}, \frac{\partial^2 \Phi}{\partial X \partial \tau}\right),$$

$$\frac{\partial \Phi}{\partial \tau} = \chi_2\left(h, \Phi, \frac{\partial h}{\partial X}, \frac{\partial q}{\partial X}, \frac{\partial \Phi}{\partial X}, \frac{\partial^2 h}{\partial X^2}, \frac{\partial^2 \Phi}{\partial X^2}\right),$$

using the solution obtained from the first step as an initial condition for the second step. The second step then returns the solution for q and Φ at the new time $\tau + \Delta\tau$.

The first step involves solving a nonlinear system of hyperbolic conservation laws which, when expressed in vector form, can be written compactly as

$$\frac{\partial \mathbf{U}}{\partial \tau} + \frac{\partial \mathbf{F}(\mathbf{U})}{\partial X} = \mathbf{B}(\mathbf{U}),$$

where

$$\mathbf{U} = \begin{bmatrix} h \\ q \\ \Phi \end{bmatrix}, \quad \mathbf{F}(\mathbf{U}) = \begin{bmatrix} q \\ \frac{9q^2}{7h} + \frac{5\cot\beta h^2}{4Re} + \frac{5M(1+So)\Phi}{4h} \\ \frac{27q\Phi}{20h} \end{bmatrix},$$

$$\mathbf{B}(\mathbf{U}) = \begin{bmatrix} 0 \\ S_1 \\ S_2 \end{bmatrix}.$$

While there are several schemes available to solve such a system, because of the complicated eigenstructure of the above system, eigen-based methods will not be practical. Instead, MacCormack's method was adopted due to its relative simplicity. This is a conservative second-order accurate finite difference scheme that correctly captures discontinuities and converges to the physical weak solution of the problem. LeVeque and Yee[44] extended MacCormack's method to include source terms via the explicit predictor-corrector scheme

$$\mathbf{U}_j^* = \mathbf{U}_j^n - \frac{\Delta\tau}{\Delta X}\left[\mathbf{F}(\mathbf{U}_{j+1}^n) - \mathbf{F}(\mathbf{U}_j^n)\right] + \Delta\tau\ \mathbf{B}(\mathbf{U}_j^n),$$

$$\mathbf{U}_j^{n+1} = \frac{1}{2}\left(\mathbf{U}_j^n + \mathbf{U}_j^*\right) - \frac{\Delta\tau}{2\Delta X}\left[\mathbf{F}(\mathbf{U}_j^*) - \mathbf{F}(\mathbf{U}_{j-1}^*)\right] + \frac{\Delta\tau}{2}\mathbf{B}(\mathbf{U}_j^*),$$

where the notation $\mathbf{U}_j^n \equiv \mathbf{U}(X_j, \tau_n)$ is utilized with ΔX denoting the uniform grid spacing and $\Delta\tau$ is the time step.

The second step reduces to solving a coupled system of generalized one-dimensional nonlinear diffusion equations with the understanding that h is determined from the first step. This system was discretized using the Crank-Nicolson scheme, whereby periodicity conditions were imposed and the output from the first step was used as an initial condition. This leads to nonlinear systems of algebraic equations which were solved iteratively. A robust algorithm taking advantage of the structure and sparseness of the resulting linearized systems was used to speed up the iterative process. It was found that convergence was reached quickly, typically in less than five iterations.

The evolution of the unsteady flow was computed by imposing a small perturbation on the constant steady-state solutions q_s, h_s, and Φ_s. If we set $q_s = 1$, then it follows that

$$h_s^5 + 12\delta h_s^4 + 54\delta^2 h_s^3 - h_s^2 - 9\delta h_s - 27\delta^2 = 0,$$

$$\Phi_s = -\frac{Bh_s^2}{(1+Bh_s)}. \tag{80}$$

We note that the algebraic equation for h_s obtained by the Navier-Stokes equations is given by (19). For small δ, the numerical solution to (80) comes in close agreement with that obtained from (19). For example, for $\delta = 0.1$, expression (80)

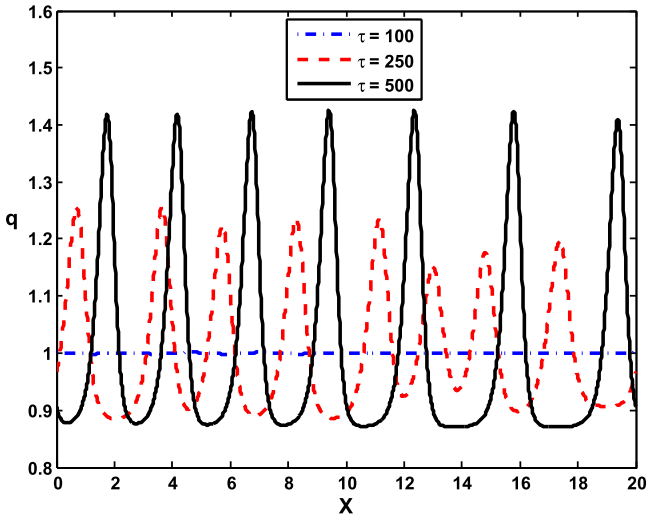

FIG. 11. Time evolution of the flow rate.

yields $h_s = 0.921$ while (19) gives $h_s = 0.909$, and for $\delta = 0.05$, (80) yields $h_s = 0.955$ while (19) gives $h_s = 0.952$. In fact, with $\delta = 0$, the two equations both yield the expected value $h_s = 1$.

By monitoring the growth of the disturbances as the perturbed solutions were marched in time, we were able to determine the stability of the flow. We carried out a simulation using the parameter values: $\cot\beta = M = 1$, $B = 4/3$, $So = 1/2$, $\mathrm{Pr} = 7$, $\delta = 0.1$, and $Re = 0.8$. The computational domain was taken to have a length of $L = 20$, the grid spacing and time step were $\Delta X = 0.01$, $\Delta\tau = 0.001$, respectively, and the small parameter ε was set to 0.1. Shown in Fig. 11 is the time evolution of the flow rate, q, which illustrates the formation of a permanent series of large amplitude waves as a result of the instability. Plotted in Fig. 12 is a snapshot of the fluid thickness, h, the surface temperature, θ, and the surface solutal concentration, C, at $\tau = 500$. It is clear that the variations in h align with the peaks in q as expected. On the other hand, the surface temperature is out of phase with the fluid thickness, that is, the surface temperature is largest when h is smallest.

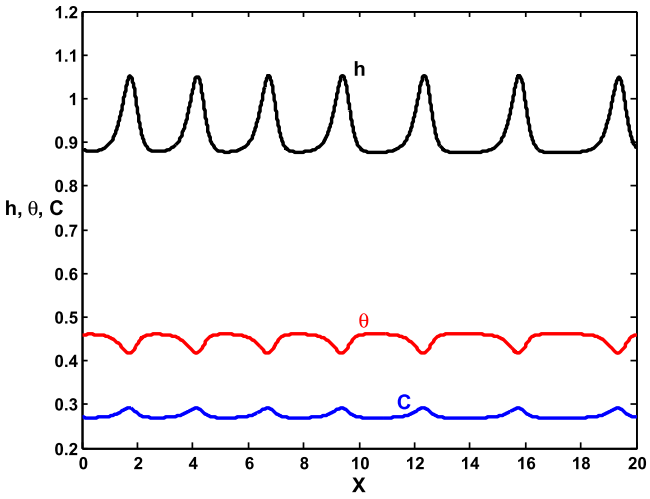

FIG. 12. The fluid thickness and surface temperature/solutal concentration at $\tau = 500$.

This is because the steady-state temperature, given by

$$T_s = 1 - \frac{B}{1 + Bh_s} z,$$

decreases linearly with z. Thus, as h increases, the surface temperature decreases. Lastly, the surface solutal concentration is shown to be out of phase with the surface temperature. This follows immediately from the relationship between the surface temperature and surface solutal concentration given by $C = So(1 - \theta)$. We note that for these parameter values, the full equations predict that the instability threshold is $Re_{crit} = 0.696$, while the linearized weighted residual equations yield an instability threshold of $Re_{crit} = 0.688$. Thus, the nonlinear simulations shown in Figs. 11 and 12 support these predictions.

V. CONCLUSIONS

In this paper, we studied the stability of the steady flow of a thin film layer with uniform thickness comprising a binary liquid mixture down a uniformly heated slippery incline. A theoretical model is employed consisting of the Navier-Stokes equations coupled with conservation equations for energy and solutal concentration. The model captures the Soret effect and implements a Navier slip condition at the liquid-solid interface with the slip length being the parameter which measures the deviation from the no-slip condition.

In carrying out a linear stability analysis, we obtained an eigenvalue problem involving the Orr-Sommerfeld-type equations governing the evolution of infinitesimal perturbations to the equilibrium flow. An asymptotic analysis of the eigenvalue problem for small perturbation wavenumbers yielded an expression for the critical Reynolds number for the instability of very long perturbations. By numerically solving the eigenvalue problem, we were able to construct the state of neutral stability for general wavenumbers and obtain the critical Reynolds number for the onset of instability of the equilibrium flow. Our primary aim has been to investigate how bottom slip interacts with the other factors affecting the stability of the flow. If the destabilizing effect of capillarity is sufficiently weak, there is an interval of Reynolds numbers for which the equilibrium flow is stable as there is sufficient inertia to stabilize the S mode, yet not enough to destabilize the H mode. In our investigation, we focused on the effect of various parameters on this region of stability. The main conclusion is that bottom slip acts as a general destabilizing factor. Specifically, the region of stability shrinks as the slip parameter is increased. Also, for a larger value of the slip parameter, the region of stability disappears sooner as the Marangoni or Soret number is increased. In other words, on a slippery surface, lower levels of thermocapillarity or destabilizing solutocapillarity are required to render the equilibrium flow unstable for all Reynolds numbers. As a consequence of this, for cases when moderately long perturbations are the most unstable, the difference in the critical Reynolds numbers between the onset of instability in the equilibrium flow and that for infinitely long perturbations becomes less pronounced.

We also considered nonlinear effects on stability by running numerical simulations of the flow by means of a reduced-dimensionality model. The obtained results are in agreement

with the predictions from the linear stability analysis for the onset of instability in the equilibrium flow. Calculations of the evolution of the flow under unstable conditions yielded a secondary flow exhibiting permanent waves. The temperature and solutal concentration distributions for this flow are found to relate to the flow rate in accordance with the physical expectations.

ACKNOWLEDGMENTS

Financial support for this research was provided by the Natural Sciences and Engineering Research Council of Canada and the Faculty of Mathematics at the University of Waterloo.

[1]P. L. Kapitza and S. P. Kapitza, "Wave flow of thin layers of a viscous fluid: III. Experimental study of undulatory flow conditions," Zh. Eksp. Teor. Fiz. **19**, 105–120 (1949).
[2]T. B. Benjamin, "Wave formation in laminar flow down an inclined plane," J. Fluid Mech. **2**, 554–574 (1957).
[3]C.-S. Yih, "Stability of liquid flow down an inclined plane," Phys. Fluids **6**, 321–334 (1963).
[4]S. Kalliadasis, E. A. Demekhin, C. Ruyer-Quil, and M. G. Velarde, "Thermocapillary instability and wave formation on a film falling down a uniformly heated plane," J. Fluid Mech. **492**, 303–338 (2003).
[5]C. Ruyer-Quil, B. Scheid, S. Kalliadasis, M. G. Velarde, and R. Kh. Zeytounian, "Thermocapillary long waves in a liquid film flow. Part 1. Low-dimensional formulation," J. Fluid Mech. **538**, 199–222 (2005).
[6]B. Scheid, C. Ruyer-Quil, S. Kalliadasis, M. G. Velarde, and R. Kh. Zeytounian, "Thermocapillary long waves in a liquid film flow. Part 2. Linear stability and nonlinear waves," J. Fluid Mech. **538**, 223–244 (2005).
[7]P. M. J. Trevelyan, B. Scheid, C. Ruyer-Quil, and S. Kalliadasis, "Heated falling films," J. Fluid Mech. **592**, 295–334 (2007).
[8]P. Kolodner, H. Williams, and C. Moe, "Optical measurement of the Soret coefficient of ethanol/water solutions," J. Chem. Phys. **88**, 6512–6524 (1988).
[9]J. K. Bhattacharjee, "Marangoni convection in binary liquids," Phys. Rev. E **50**, 1198–1205 (1994).
[10]S. W. Joo, "Marangoni instabilities in liquid mixtures with Soret effect," J. Fluid Mech. **293**, 127–145 (1995).
[11]A. Podolny, A. Oron, and A. A. Nepomnyashchy, "Long-wave Marangoni instability in a binary-liquid layer with deformable interface in the presence of Soret effect: Linear theory," Phys. Fluids **17**, 104104 (2005).
[12]A. Podolny, A. Oron, and A. A. Nepomnyashchy, "Linear and nonlinear theory of long-wave Marangoni instability with the Soret effect at finite Biot numbers," Phys. Fluids **18**, 054104 (2006).
[13]A. Podolny, A. Oron, and A. A. Nepomnyashchy, "Long-wave Marangoni instability in a binary liquid layer on a thick solid substrate," Phys. Rev. E **76**, 026309 (2007).
[14]M. Morozov, A. Oron, and A. A. Nepomnyashchy, "Nonlinear dynamics of long-wave Marangoni convection in a binary mixture with the Soret effect," Phys. Fluids **25**, 052107 (2013).
[15]J. Hu, H. Ben Hadid, D. Henry, and A. Mojtabi, "Linear temporal and spatio-temporal stability analysis of a binary liquid film flowing down an inclined uniformly heated plate," J. Fluid Mech. **599**, 269–298 (2008).
[16]J. P. Pascal and S. J. D. D'Alessio, "Thermosolutal Marangoni effects on the inclined flow of a binary liquid with variable density. I. Linear stability analysis," Phys. Rev. Fluids **1**, 083603 (2016).
[17]S. J. D. D'Alessio and J. P. Pascal, "Thermosolutal Marangoni effects on the inclined flow of a binary liquid with variable density. II. Nonlinear analysis and simulations," Phys. Rev. Fluids **1**, 083604 (2016).
[18]C. L. M. H. Navier, "Memoire sur les lois du mouvement des fluides," Mem. Acad. R. Sci. Inst. France **6**, 389–440 (1823).
[19]J. P. Rothstein, "Slip on superhydrophobic surfaces," Annu. Rev. Fluid Mech. **42**, 89–109 (2010).
[20]V. S. Ajaev, *Interfacial Fluid Mechanics: A Mathematical Modeling Approach* (Springer, New York, 2012).
[21]G. S. Beavers and D. D. Joseph, "Boundary conditions at a naturally permeable wall," J. Fluid Mech. **30**, 197–207 (1967).
[22]J. P. Pascal, "Linear stability of fluid flow down a porous inclined plane," J. Phys. D **32**, 417–422 (1999).
[23]R. Liu and Q. S. Liu, "Instabilities of a liquid film flowing down an inclined porous plane," Phys. Rev. E **80**, 036316 (2009).
[24]I. M. R. Sadiq, R. Usha, and S. Joo, "Instabilities in a liquid film flow over an inclined heated porous substrate," Chem. Eng. Sci. **65**, 4443 (2010).
[25]M. Sellier, "Substrate design or reconstruction from free surface data for thin film flows," Phys. Fluids **20**, 062106 (2008).
[26]C. Heining and N. Aksel, "Bottom reconstruction in thin-film flow over topography: Steady solutions and linear stability," Phys. Fluids **21**, 083605 (2009).
[27]R. Usha and Anjalaiah, "Steady solution and spatial stability of gravity-driven thin-film flow: Reconstruction of an uneven slippery bottom substrate," Acta Mech. **227**, 1685–1709 (2016).
[28]Anjalaiah and R. Usha, "Effects of velocity slip on the inertialess instability of a contaminated two-layer film flow," Acta Mech. **226**, 3111–3132 (2015).
[29]S. Ghosh and R. Usha, "Stability of viscosity stratified flows down an incline: Role of miscibility and wall slip," Phys. Fluids **28**, 104101 (2016).
[30]J. P. Pascal, N. Gonputh, and S. J. D. D'Alessio, "Long-wave instability of flow with temperature dependent fluid properties down a heated incline," Int. J. Eng. Sci. **70**, 73–90 (2013).
[31]S. J. D. D'Alessio, C. J. M. P. Seth, and J. P. Pascal, "The effects of variable fluid properties on thin film stability," Phys. Fluids **26**, 122105 (2014).
[32]L. N. Trefethen, *Spectral Methods in MATLAB* (SIAM, Philadelphia, 2000).
[33]I. S. Khattab, F. Bandarkar, M. A. A. Fakhree, and A. Jouyban, "Density, viscosity, and surface tension of water+ethanol mixtures from 293 to 323 K," Korean J. Chem. Eng. **29**, 812–817 (2012).
[34]S. Kalliadasis, C. Ruyer-Quil, B. Scheid, and M. G. Velarde, *Falling Liquid Films* (Springer-Verlag, London, UK, 2012).
[35]A. Samanta, C. Ruyer-Quil, and B. Goyeau, "A falling film down a slippery inclined plane," J. Fluid Mech. **684**, 353–383 (2011).
[36]D. A. Nield and A. Bejan, *Convection in Porous Media*, 3rd ed. (Springer, New York, 2006).
[37]C. Ruyer-Quil and P. Manneville, "Improved modeling of flows down inclined planes," Eur. Phys. J. B **15**, 357–369 (2000).
[38]C. Ruyer-Quil and P. Manneville, "Further accuracy and convergence results on the modeling of flows down inclined planes by weighted-residual approximations," Phys. Fluids **14**, 170–183 (2002).
[39]S. J. D. D'Alessio, J. P. Pascal, and H. A. Jasmine, "Instability in gravity-driven flow over uneven surfaces," Phys. Fluids **21**, 062105 (2009).
[40]J. P. Pascal and S. J. D. D'Alessio, "Instability in gravity-driven flow over uneven permeable surfaces," Int. J. Multiphase Flow **36**, 449–459 (2010).
[41]S. J. D. D'Alessio, J. P. Pascal, H. A. Jasmine, and K. A. Ogden, "Film flow over heated wavy inclined surfaces," J. Fluid Mech. **665**, 418–456 (2010).
[42]K. A. Ogden, S. J. D. D'Alessio, and J. P. Pascal, "Gravity-driven flow over heated, porous, wavy surfaces," Phys. Fluids **23**, 122102 (2011).
[43]R. J. LeVeque, *Finite Volume Methods for Hyperbolic Problems* (Cambridge University Press, Cambridge, 2002).
[44]R. J. LeVeque and H. C. Yee, "A study of numerical methods for hyperbolic conservation laws with stiff source terms," J. Comput. Phys. **86**, 187–210 (1990).